energies

MDPI

Article

Experimental Analysis and Optimization of an R744 Transcritical Cycle Working with a Mechanical Subcooling System

Daniel Sánchez *, Jesús Catalán-Gil, Ramón Cabello, Daniel Calleja-Anta, Rodrigo Llopis and Laura Nebot-Andrés

Department of Mechanical Engineering and Construction, Jaume I University, E-12071 Castellón, Spain; jcatalan@uji.es (J.C.-G.); cabello@uji.es (R.C.); calleja@uji.es (D.C.-A.); rllopis@uji.es (R.L.); lnebot@uji.es (L.N.-A.)

* Correspondence: sanchezd@uji.es; Tel.: +34-964728142

Received: 10 May 2020; Accepted: 11 June 2020; Published: 19 June 2020

Abstract: In the last century, the refrigerant R744 (carbon dioxide) has become an environmentally friendly solution in commercial refrigeration despite its particular issues related to the low critical temperature. The use of transcritical cycles in warm and hot countries reveals the necessity of adopting different configurations and technologies to improve this specific cycle. Among these, subcooling methods are well-known techniques to enhance the cooling capacity and the Coefficient of Performance (COP) of the cycle. In this work, an R600a dedicated mechanical subcooling system has been experimentally tested in an R744 transcritical system at different operating conditions. The results have been compared with those obtained using a suction-to-liquid heat exchanger (IHX) to determine the degree of improvement of the mechanical subcooling system. Using the experimental tests, a computational model has been developed and validated to predict the optimal subcooling degree and the cubic capacity of the mechanical subcooling compressor. Finally, the model has been used to analyze the effect of using different refrigerants in the mechanical subcooling unit finding that the hydrocarbon R290 and the HFC R152a are the most suitable fluids.

Keywords: R744; CO_2; transcritical; subcooling; IHX; R600a; R290; R152a; R1234yf

1. Introduction

In recent years, carbon dioxide (CO_2) has been established as a sustainable working fluid in commercial refrigeration encouraged not only for its environmental friendless, high-security classification and excellent properties but also because it is a natural substance with an extensive background in the industry. CO_2 offers an ultra-low Global Warming Potential (GWP) which contributes positively to reduce the environmental impact caused by refrigeration plants when the refrigerant is released to the atmosphere (direct effect). However, the whole environmental effect of these facilities also depends on the carbon dioxide emissions associated with the production of the electricity consumed by these systems. Regarding this, CO_2 has an important drawback related to its low critical temperature around 31 °C). This temperature forces the system to operate under transcritical conditions which increases the power consumption and the exergy losses especially during the throttling process [1,2]. The main consequence of this particular behaviour is the low COP of the system in warm and hot climates compared to conventional hydrofluorocarbon (HFC) arrangements. For cooler climates, (e.g., northern Europe), the use of CO_2 is preferred in supermarkets because its COP exceeds conventional HFC-systems [3,4]. Moreover, it offers the possibility of heat recovering and integrating air conditioning [5–7]. According to the last report presented by Shecco [8], almost 84.5% of the CO_2 transcritical supermarkets installed in Europe are located in Germany, the UK, Norway, Denmark, Sweden and Switzerland.

In order to improve the Coefficient of Performance (COP) of CO_2 transcritical cycles, several modifications have been made in the basic transcritical cycle over the years. Thus, the works published by Tsamos et al. [9], Gullo et al. [10], Haida et al. [11], Purohit et al. [12], Karampour et al. [13], Catalán-Gil et al. [14,15], Mitsopoulos et al. [16] or Bellos and Tzivanidis [17], among others, explain how transcritical booster cycles can be improved by using different strategies such as the parallel compressor, the mechanical subcooler system, the multi-ejector concept or the overfed evaporators. Other solutions are focused on taking advantage of the wasted heat from transcritical cycles by obtaining hot water [18], activating absorption systems [19,20] or using it in a desiccant-wheel in an air conditioning system [21].

The mechanical subcooler system (referred to as MS system henceforth) consists of a vapour compression cycle coupled to the transcritical system by means of a heat exchanger named subcooler. This heat exchanger reduces the temperature of CO_2 at the exit of the gas-cooler just before entering the back-pressure valve, providing an increment in the cooling capacity of the refrigerating plant. As a consequence, the use of the MS system could reduce the CO_2 compressor size if a specific cooling capacity is desired reducing the total power consumption of the refrigerating plant [22,23].

Since the first report in 1973 by Brown [24], several authors have analysed the use of the mechanical subcooling system to improve the operation of commercial refrigeration plants [25–28] and also, air-conditioning systems [29–31]. However, the first report that proposes the use of this system for CO_2 transcritical systems was presented in 2012 by Brouwers and Serwas [32] and implemented at the end of 2013 in a hypermarket located in Alzira (Spain) [33]. From a theoretical point of view, She et al. [34] analyzed the use of a mechanical subcooling cycle driven by the power recovered from an expander installed in the main CO_2 cycle. This new arrangement improved the facility's COP by up to 65% regarding the cycle without subcooling. Hafner and Hemmingsen [35] suggested and quantified different options to improve an R744 booster system operating at high ambient temperatures. Taking an R404A direct expansion system as a reference, the MS system reported benefits in terms of COP up to 28.6% (at low ambient temperatures), and similar values at high ambient temperatures compared to the basic system without subcooling. Llopis et al. [36] presented a theoretical analysis of the potential improvement of a transcritical cycle working with a dedicated mechanical subcooling. Using three different subcooling degrees and a range of ambient temperatures from 20 to 35 °C, the work reported new results that supported the conclusions drawn from the previous studies.

Sánchez et al. [37] experimentally analysed the use of an R600a MS system in a small CO_2 transcritical refrigerating plant. The results at a fixed evaporating temperature of −10 °C and heat-rejection conditions of 35 °C, showed improvements of up to 40.9% in terms of cooling capacity and up to 17.3% in the optimal COP, taking a single-stage transcritical cycle without IHX as a reference. Furthermore, the use of the MS system reduced the optimal heat rejection pressure by approx. 3 bar. Similarly, Nebot-Andrés et al. [38] experimentally analyzed the impact of using an MS system with R1234yf in a CO_2 transcritical refrigerating plant previously tested by Cabello et al. [39]. The results obtained at a heat-rejection temperature of 30 °C and an evaporating level of 0 °C reported a maximum increment of 22.8% in terms of COP and cooling capacity enhancement of 34.9% compared to the cycle without subcooling. Moreover, the authors remarked a reduction in the optimal heat rejection pressure of 8.8 bar. Mazzola et al. [22] presented a semi-empirical study whit three different subcooling systems used for supermarkets: groundwater, water from an A/C system and an MS system. The results demonstrated that all the subcooling systems were able to reduce the heat-rejection pressure and gave energy savings between 25% and 36% using the system without subcooling as a reference.

Eikevik et al. [40] tested a transcritical refrigerating plant with an MS system using R290 as a refrigerant. The system included a gas-cooler with an integrated propane condenser which, depending on the heat-rejection temperatures, provided increments from 8.8% to 6.9% at ambient temperatures of 18.7 °C and 40 °C, respectively. Bush et al. [41] experimentally tested a CO_2 two-stage refrigeration system under laboratory conditions using an indirect MS system with R134a. The results obtained for the evaporative levels of −7 and −28 °C and several temperatures for the heat rejection, demonstrated a substantial COP improvement from 10 to 15% depending on the load ratio compared with the

refrigeration system without indirect subcooling. Dai et al. [42] published a theoretical assessment that evidences the existence of an optimum subcooling degree that maximizes the COP of the refrigerating facility. Later, Dai et al. [43] demonstrate that the use of zeotropic mixtures with a proper glide in the MS system could provide an increment of up to 4.91% over the pure fluids, especially at high ambient temperatures. Finally, Liu et al. [44] provided a complete analysis of different positions for the mechanical subcooling system in a CO_2 booster-system using R290 as the refrigerant in the auxiliary unit.

In the light of the research presented above, there are multiple options for the refrigerant used in the mechanical subcooling unit that can enhance the performance of the base cycle. However, few studies are comparing these refrigerants to maximize the COP of the system. Focusing on that, this works aims to compare the operation of a transcritical system upgraded with a mechanical subcooling unit using different refrigerants. To do this, an R744 transcritical refrigerating plant has been tested with a suction-to-liquid heat exchanger and an R600a dedicated mechanical subcooling unit. Then, the experimental results have been analyzed and discussed, obtaining the key parameters to develop a computational model validated with the experimental tests. Finally, this model has been used to maximize the COP of the plant by optimizing the mechanical subcooling system using the low-GWP refrigerants in accordance with the Regulation EU No 517/2014: R600a, R290, R152a and R1234yf. The experimental analysis was performed in a wide range of heat-rejecting temperatures from 20 to 40 °C at the evaporating levels of 0 and −10 °C, although the computational optimization has been performed at −10 °C typically used in commercial refrigeration.

2. Experimental Apparatus

2.1. Refrigeration Facility

The experimental facility used in this work is equipped with different configurations that can be tested individually by using the by-passes installed in the refrigerating plant. Figure 1 details the schematic diagram of the refrigerating plant and the arrangements of (a) Base cycle, (b) IHX cycle, and (c) MS cycle.

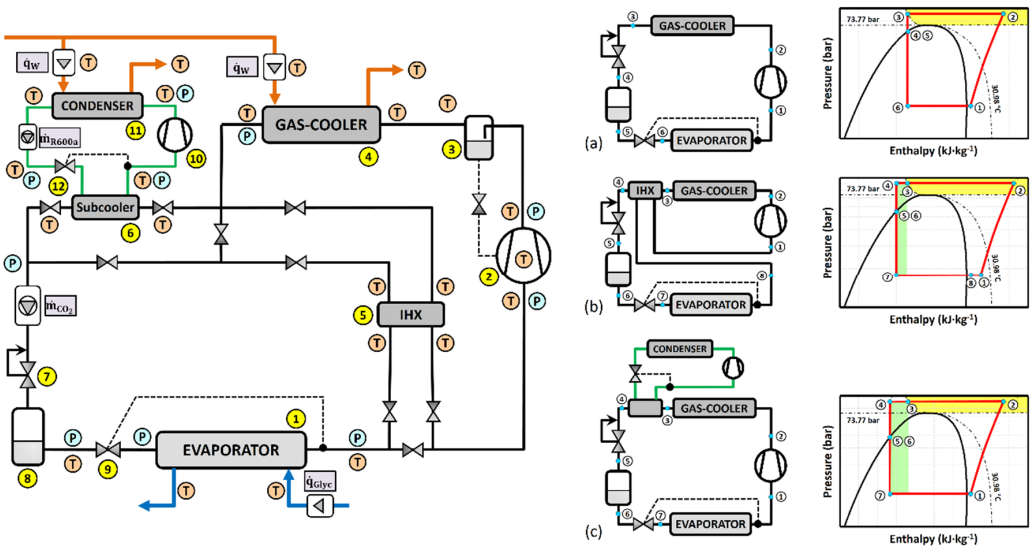

Figure 1. Schematic diagram of the experimental refrigeration plant including the analyzed configurations: (**a**) Base cycle, (**b**) IHX cycle and (**c**) MS cycle.

According to Figure 1, the experimental facility consists of a single-stage vapour compression cycle equipped with a brazed-plate evaporator (1) with a heat transfer area of 0.576 m^2; a hermetic-compressor (2) with a cubic capacity ($V_{g.CO2}$) of 1.75 cm^3 and a rotation speed (N) of 2900 rpm; a coalescing oil

separator (3); a brazed-plate gas-cooler/condenser (4) with a heat transfer area of 0.576 m^2; a tube-in-tube suction-to-liquid heat exchanger (5) with a heat transfer area of 0.022 m^2; a brazed-plate subcooler (6) with a heat transfer area of 0.216 m^2; and finally, a double-stage throttling system with an electronic back-pressure valve (7), a liquid receiver of 3.7 litres (8) and a thermostatic expansion valve (9). The mechanical subcooling unit is composed of an R600a hermetic compressor (10) with a cubic capacity ($V_{g.MS}$) of 2.72 cm^3 and a rotation speed (N) of 2900 rpm; a brazed-plate condenser (11) with a heat transfer area of 0.216 m^2; and finally, a thermostatic expansion valve (12). To minimise the heat exchange with the environment, all pipes were insulated with a foam of low thermal conductivity (0.036 $W{\cdot}m^{-1}{\cdot}K^{-1}$).

The main fluids used to test the facility were carbon dioxide (R744) in the main circuit and isobutene (R600a) in the mechanical subcooling unit. The secondary fluids were water in the gas-cooler and condenser, and a mixture of water and propylene-glycol (70/30% by mass) in the evaporator of the main circuit.

Data from the refrigeration plant were acquired with different measurement devices detailed in Table 1 connected to a data acquisition system (DAQ) with a registered time of 10 s for a minimum 15-min period. The information from DAQ was recorded by a personal computer, and the thermophysical properties of the refrigerants and secondary fluids were calculated by the RefProp v.9.1 software [45] and ASHRAE correlations [46], respectively.

Table 1. Accuracies and calibration range of the measurement devices.

Number	Measured Variable	Measuring Device	Calibration Range	Accuracy
24	Temperature (°C)	T-type thermocouple	−40.0 to 125.0 °C	±0.5 K
3	Pressure (CO_2 cycle)	Pressure gauge	0.0 to 160.0 bar	±0.6% of span
1	Pressure (CO_2 cycle)	Pressure gauge	0.0 to 100.0 bar	±0.6% of span
3	Pressure (CO_2 cycle)	Pressure gauge	0.0 to 60.0 bar	±0.6% of span
2	Pressure (MS cycle)	Pressure gauge	0.0 to 16.0 bar	±0.25% of spam
1	Pressure (MS cycle)	Pressure gauge	0.0 to 9.0 bar	±0.25% of span
1	Glycol volume flow rate	Magnetic flow meter	0.0 to 4.0 $m^3{\cdot}h^{-1}$	±0.25% of reading
1	Water volume flow rate	Magnetic flow meter	0.0 to 4.0 $m^3{\cdot}h^{-1}$	±0.25% of reading
2	Refrigerant mass flow rate	Coriolis mass flow meter	0.0 to 0.1 $kg{\cdot}s^{-1}$	±0.1% of reading
1	Power consumption (CO_2 cycle)	Network analyser	0.0 to 2000.0 W	±0.5% of reading
1	Power consumption (MS cycle)	Network analyser	0.0 to 200.0 W	±0.5% of reading

To obtain more precise readings on temperature especially at the exit of the gas-cooler or evaporator, some temperature probes were installed inside the refrigeration facility with immersion thermocouples. The remaining probes were installed over the pipes and insulated from the environment with a foam.

From the information summarized in Table 1, the experimental uncertainty of the indirect measurements can be determined using the propagation of error described by Moffat [47], which includes the standard deviation during tests and the accuracy of the measurement devices. Table 2 gathers the range of these uncertainties for the cooling capacity, the total power consumed by the refrigeration plant, the subcooling degree and the COP.

Table 2. Uncertainty range for the indirect measured variables.

Cycle	$\dot{Q}_{o.co2}$ (W)	$\dot{W}_{plant}$ (W)	ΔT_{SUB} (K)	COP
Base cycle	± (3.6 ÷ 6.3)	± (1.8 ÷ 2.6)	-	± (0.01 ÷ 0.04)
IHX cycle	± (3.3 ÷ 8.5)	± (1.9 ÷ 2.7)	± (0.3 ÷ 0.4)	± (0.01 ÷ 0.05)
MS cycle	± (4.3 ÷ 10.5)	± (1.8 ÷ 2.5)	± (0.3 ÷ 0.5)	± (0.01 ÷ 0.08)

2.2. Test Methodology

To evaluate the performance of the experimental plant, 96 tests were performed within a wide range of operating conditions. Table 3 summarises the values of the parameters used as a reference.

The useful superheating of the main cycle (SH_{CO2}) and the mechanical subcooling system (SH_{R600a}) was set to 3.5 K by the thermostatic valve.

Table 3. Reference parameters.

Cycle	$T_{O,CO2}$ (°C)	$T_{W.in}$ (°C)	P_{GC-K} (bar)	$\dot{q}_W$ (m^3/h)	$\dot{q}_{Glyc}$ (m^3/h)	SH_{CO2} (K)	SH_{R600a} (K)
Base cycle MS cycle	−10 °C 0 °C	35 °C 30 °C 25 °C 20 °C	100 to P_{min} 100 to P_{min} 80 to P_{min} 80 to P_{min}	0.2 m^3/h	0.2 m^3/h	3.5 K	3.5 K
IHX cycle	−10 °C 0 °C	35 °C 30 °C	100 to P_{min} 100 to P_{min}	0.2 m^3/h	0.2 m^3/h	3.5 K	-

The heat rejection pressure (P_{GC-K}) was ranged from 100 or 80 bar to a minimal pressure (P_{min}) defined by the heat rejection temperature. Thus, for temperatures of 35 and 30 °C, the minimal heat rejection pressure depends on the liquid receiver pressure (8) which value must be lower than the critical pressure (73.8 bar). This limitation is made to assess the stability of the cycle. For the temperatures of 20 and 25 °C, the minimal pressure depends on the configuration adopted. The Base cycle has a minimum pressure defined by the condensing pressure when the back-pressure valve (7) is fully opened. However, in the mechanical subcooling system, the minimal pressure is defined as the theoretical condensing pressure at the heat rejection temperature, plus an increment of 4 bar to overcome the effect of the liquid receiver. Otherwise, if the back-pressure valve will be left fully open, the liquid receiver will inhibit the subcooling effect and it will force the subcooler (6) to work as an extended part of the condenser. Under these conditions, the experimental tests demonstrated that the mechanical subcooling system penalized the COP of the refrigerating plant due to the increment of its power consumption. Due to this, the minimal pressure has been limited.

2.3. Data Validation

The variables of cooling capacity ($\dot{Q}_O$), heat rejection capacity ($\dot{Q}_{GC-K}$) and subcooling effect from the mechanical subcooling system ($\dot{Q}_{MS}$), can be calculated by either the main refrigerant (CO_2) or the secondary fluid (water and propylene-glycol, water or R600a, respectively). A comparison between both allows us to check the proper operation of the refrigeration facility and the data acquisition system as well as the correct thermophysical property calculation. Equations (1)–(6) show how thermal powers have been calculated and Figure 2 depicts the average values obtained from these equations with the standard deviation as bar error.

$$\dot{Q}_{O.CO2} = \dot{m}_{CO2} \cdot (h_{O,CO2,out} - h_{O,CO2,in}) \quad (1)$$

$$\dot{Q}_{O.Glyc} = \frac{\dot{q}_{Glyc}}{3600} \cdot \rho_{Glyc,in} \cdot c_{P,Glyc} \cdot \left(T_{Glyc,in} - T_{Glyc,out}\right) \quad (2)$$

$$\dot{Q}_{GC-K,CO2} = \dot{m}_{CO2} \cdot (h_{GC-K,CO2,in} - h_{GC-K,CO2,out}) \quad (3)$$

$$\dot{Q}_{GC-K.W} = \frac{\dot{q}_{W2}}{3600} \cdot \rho_{W,in} \cdot c_{P,W} \cdot (T_{W,out} - T_{W,in}) \quad (4)$$

$$\dot{Q}_{MS} = \dot{m}_{MS} \cdot (h_{MS,out} - h_{MS,in}) \quad (5)$$

$$\dot{Q}_{MS.CO2} = \dot{m}_{CO2} \cdot (h_{MS,CO2,in} - h_{MS,CO2,out}) \quad (6)$$

According to Figure 2, the maximum deviations recorded for $\dot{Q}_o$, $\dot{Q}_{GC-K}$ and $\dot{Q}_{MS}$, were 12.0%, 10.9% and 12.7%, respectively. These deviations were obtained when the refrigeration facility operates near the pseudocritical point described by Liao and Zhao [48] and experimentally proved by Torrella et al. [49]. At this point, thermophysical properties (and especially specific heat at constant

pressure) vary drastically with temperature, affecting the heat transfer coefficients and consequently the calculation accuracy. The rest of the experimental data showed deviations lower than 7% for 89.2% for all the measured data, so the measurement system can be assumed as valid.

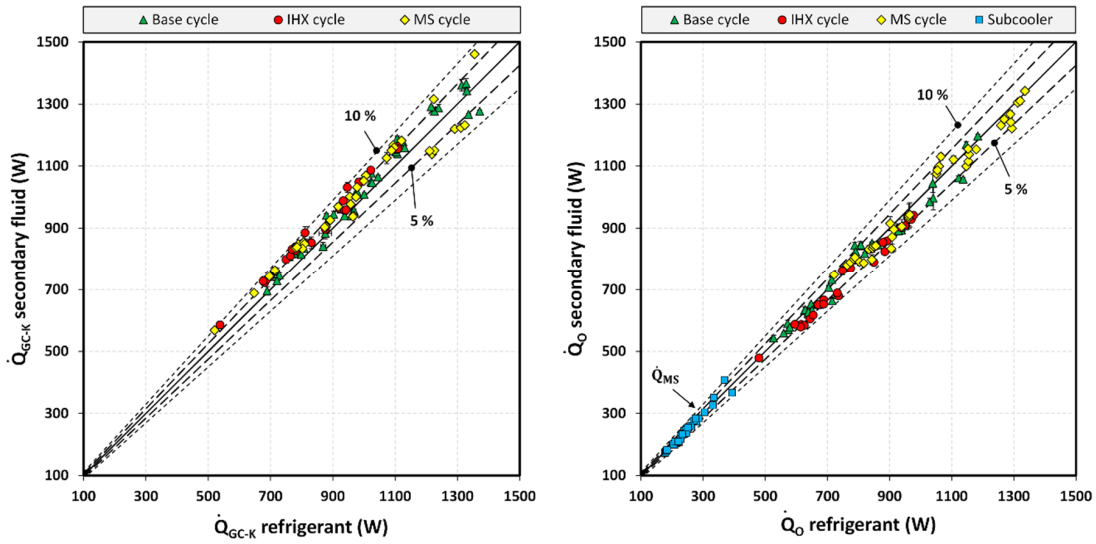

(**a**) (**b**)

Figure 2. Experimental data validation: (**a**) cooling capacity (**b**) heat rejection power and subcooler capacity.

3. Experimental Analysis

3.1. Discharge Temperature

The main variables to affect the discharge temperatures are the temperature and the pressure at the compressor suction port, and the discharge pressure. Since the mechanical subcooling unit does not affect the inlet conditions of the CO_2 compressor, the discharge temperature will remain similar to the Base cycle. However, the use of the IHX modifies the suction temperature and, consequently, the discharge temperature will change. Figure 3 shows how the discharge temperature is affected by the configuration used at the evaporating temperatures of 0 and −10 °C.

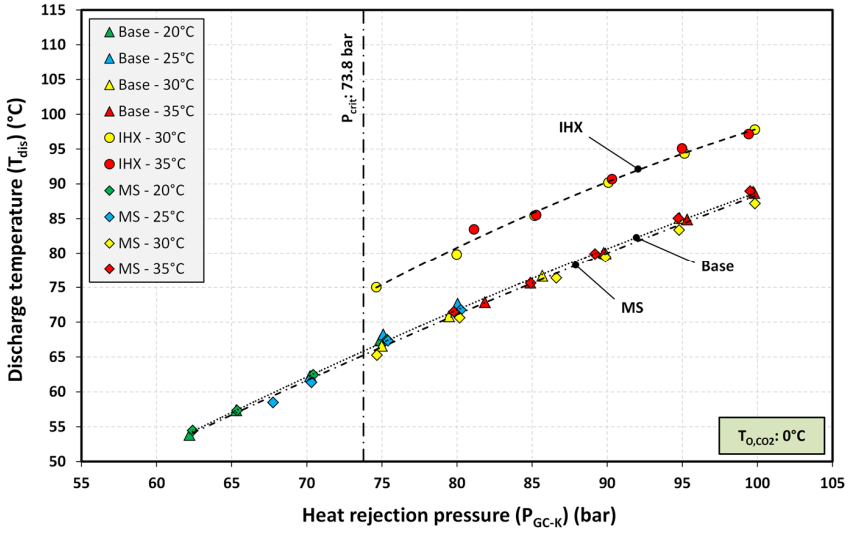

(**a**)

Figure 3. *Cont.*

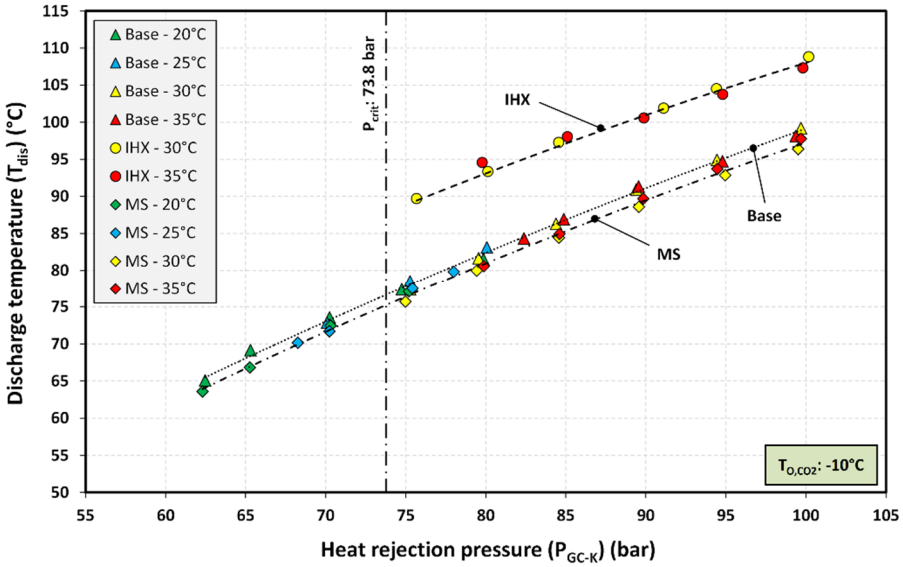

(**b**)

Figure 3. Average discharge temperature (T_{dis}) of the refrigerating plant at 0 °C (**a**) and −10 °C (**b**).

From the experimental results, it is demonstrated that the effect of the mechanical subcooling in the discharge temperature is negligible. The small variation presented in Figure 3 (from 0.4 to 2 K) is due to the control of the useful superheating. Regarding the IHX, its use modifies the suction temperature increasing the discharge temperature from +8.3 to +10.4 K concerning the Base cycle. This behaviour is following the experimental results obtained by Torrella et al. [49] and Purohit et al. [50]. As a result, the discharge temperature rises to 105 °C at the evaporating level of −10 °C.

3.2. Electrical Power Consumption

Figure 4 presents the average power consumption of the refrigerating plant excluding the auxiliary consumptions of secondary fluids pumps or control devices. The deviation during tests is presented as bar errors which value is very small. The use of an R600a mechanical subcooling unit adds extra power consumption rated from +9.3 to +22.2% concerning the base-cycle. These results are under the experimental results by Nebot-Andrés et al. [38] which increments were ranged from 17.6 to 19.0%. Taking into account that the present study is performed with a non-optimized MS cycle, it is expected that the power consumed by the refrigerating plant will be reduced if the subcooling degree is optimized and a suitable refrigerant is selected.

Concerning the IHX, it hardly affects the input power consumption despite its influence on the refrigerant mass flow rate and the specific compressor work. The effect of the IHX over the electrical power consumption ranges from +6.0 to −3.7 W. The results are supported by those presented by Sánchez et al. [51].

3.3. Cooling Capacity

Cooling capacity is obtained by Equation (2) as a product between the mass flow rate driven by the CO_2 compressor ($\dot{m}_{CO2}$) and the specific cooling capacity in the evaporator. Since the superheating degree at the evaporator is maintained by the thermostatic valve, the enthalpy at the evaporator outlet remains constant and the provided cooling capacity depends on both, the refrigerant mass flow rate and the enthalpy at the evaporator inlet. The mass flow rate is hardly affected by the presence of the mechanical subcooling unit because the pressure ratio is set externally and the properties at the compressor suction port do not vary. However, the use of IHX introduces extra superheating that implies a mass flow reduction depending on the operating conditions [49,50]. Regarding the enthalpy

evaporator inlet, the use of both subcooling systems lowers the temperature at the back-pressure valve inlet so the specific cooling capacity will be increased if an isenthalpic process is assumed in both expansion devices.

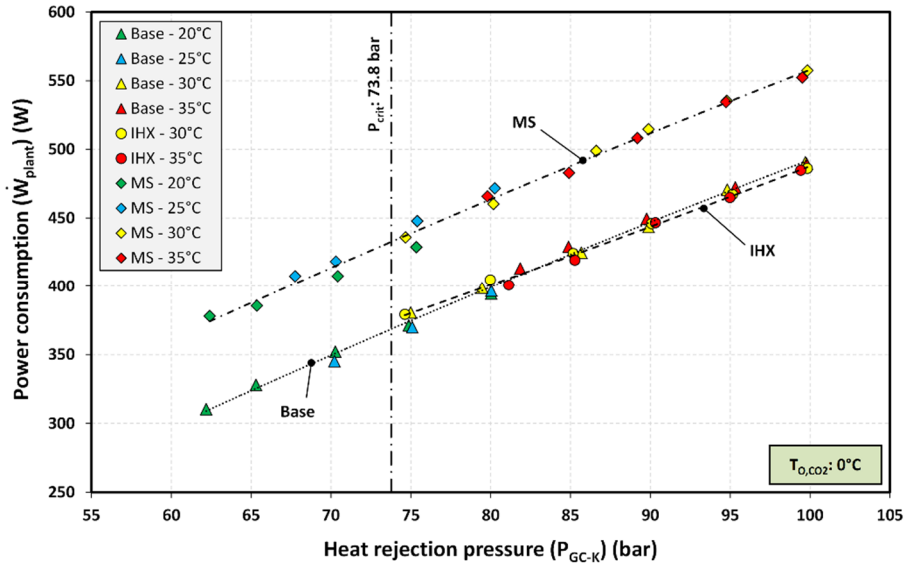

(**a**)

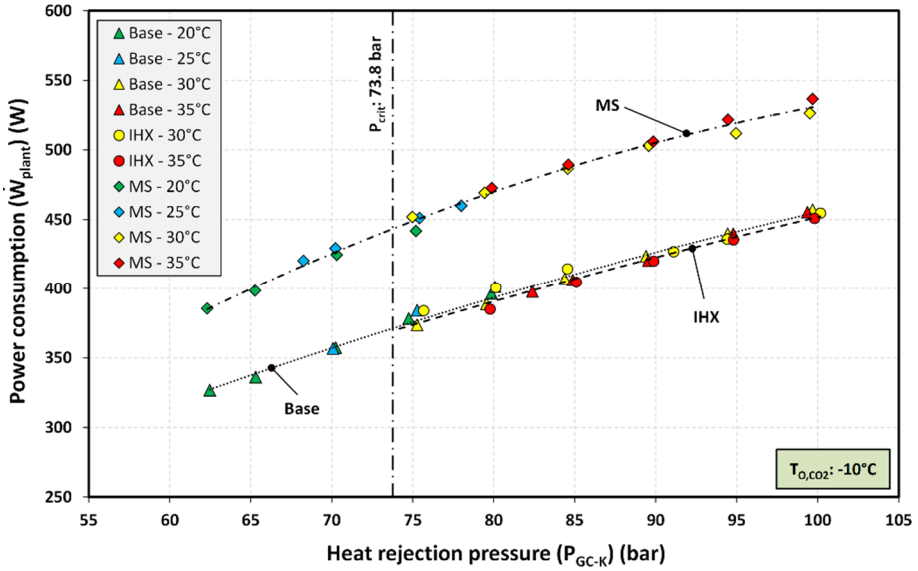

(**b**)

Figure 4. Average power consumption ($\dot{W}_{plant}$) of the refrigerating plant at 0 °C (**a**) and −10 °C (**b**).

Figure 5 presents the average cooling capacity obtained from tests. It is evidenced that the presence of an IHX or a mechanical subcooling unit always report a positive effect over the cooling capacity especially at high-rejection temperatures and lower evaporating pressure. Thus, the increments about the Base cycle are rated between +0.9 and +11.0% at 0 °C, and from +2.3 to +9.0% at −10 °C when the IHX is used. For the MS cycle, the experimental data report an increment from +12.7 to +38.9% at 0 °C, and from +16.6 to +46.4% at −10 °C. Notwithstanding, it is important to remark that the effective increment of cooling capacity is commonly obtained at the optimal conditions of COP because that is the desired operating point. This optimal conditions will describe in the next section.

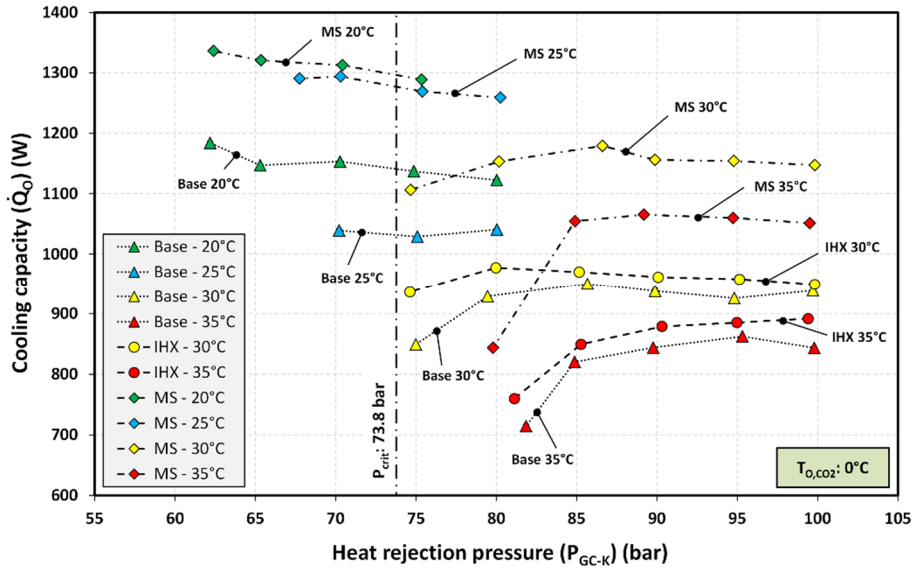

(**a**)

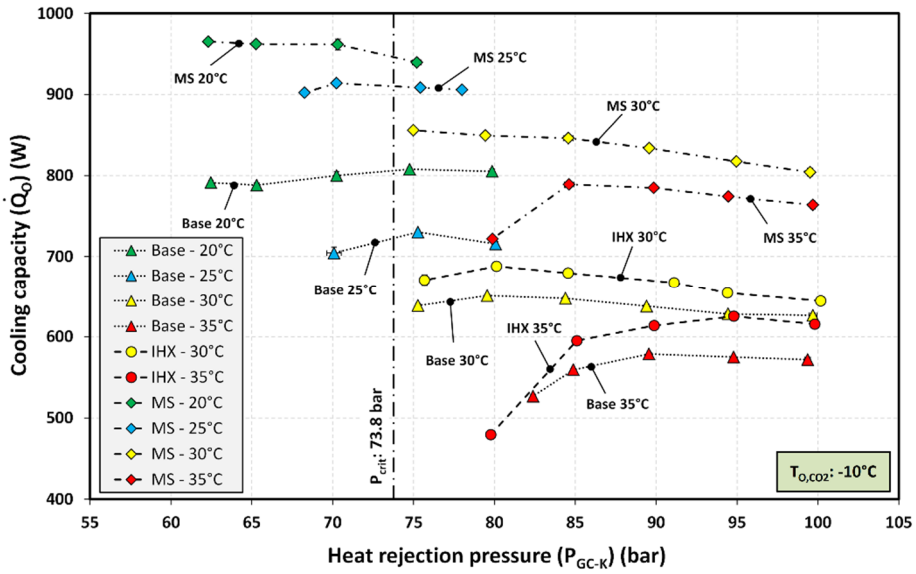

(**b**)

Figure 5. Average cooling capacity ($\dot{Q}_O$) of the refrigerating plant at 0 °C (**a**) and −10 °C (**b**).

3.4. COP

The parameter of COP is defined by Equation (7) as the ratio between the cooling capacity ($\dot{Q}_{O.CO2}$) and the input power used by the plant. This last excludes the pumping energy used to move the water through the heat exchangers

$$COP = \frac{\dot{Q}_{O.CO2}}{\dot{W}_{plant}} = \frac{\dot{m}_{CO2} \cdot (h_{O,CO2,out} - h_{O,CO2,in})}{\sum \dot{W}_{C_i}} \quad (7)$$

Figure 6 presents the average COP for the evaporating temperatures of 0 and −10 °C at the different heat-rejection temperatures. Taking the Base cycle as a reference, it can be affirmed that the subcooling effect enhances the COP of the refrigeration facility especially at high-rejection temperatures and low evaporating levels. These results are in agreement with those published by Torrella et al. [49] and

Nebot-Andrés et al. [38] at the heat-rejection temperatures of 30 and 35 °C. However, for temperatures below 30 °C, there is no experimental data published up to now that evidence the suitability of using the MS system taking the COP as a reference. Accordingly, the results depicted in Figure 6 evidence that for 20 °C the MS cycle is unsuitable because the COP of the modified system is similar to or lower than the Base cycle. For 25 °C, only at the evaporating level of −10 °C the use of the MS cycle reports a COP greater than the Base cycle.

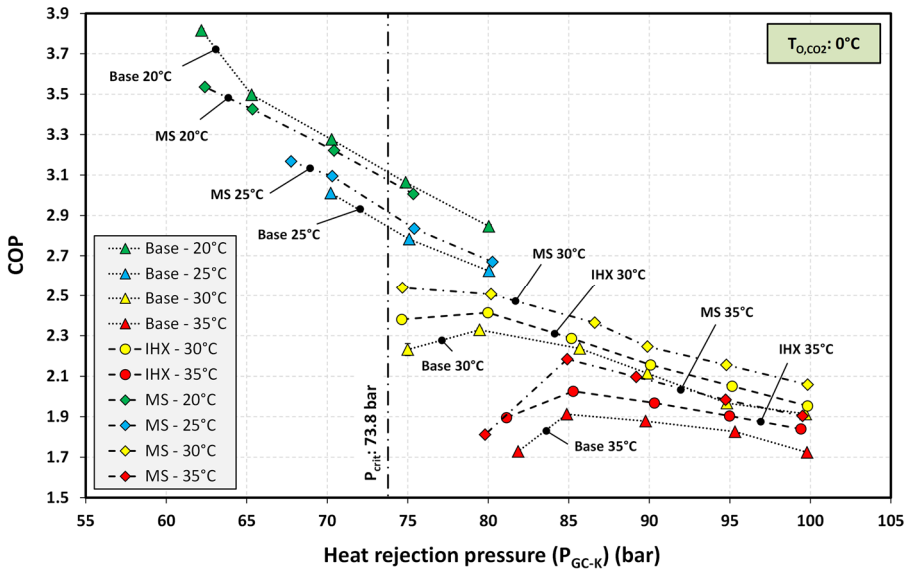

(**a**)

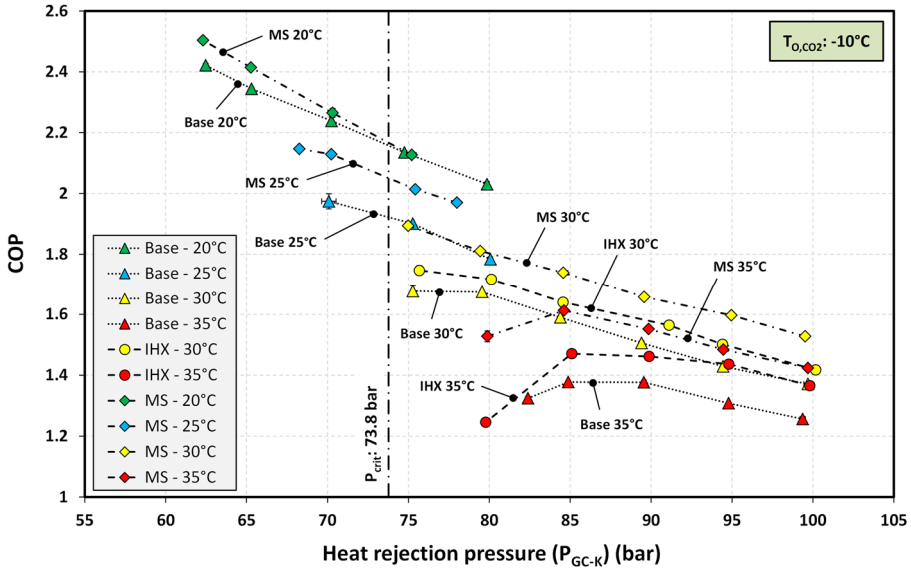

(**b**)

Figure 6. Average COP of the refrigerating plant at 0 °C (**a**) and −10 °C (**b**).

Because transcritical cycles are normally designed to operate with the maximum COP, Table 4 provides the values of the energy parameters at this operation point. The most representative parameter to fix the maximum COP is the heat rejection pressure which is commonly called optimum pressure ($P_{GC-K.opt}$) [52]. This pressure included in Table 4 is obtained by the least-square best-fit method using the experimental data. Once the optimum pressure is determined, the energy parameters are estimated by a linear interpolation method.

Table 4. Adjusted results at optimal operating conditions.

$T_{O,CO2}$ (°C)	$T_{W.in}$ (°C)	$P_{GC\text{-}K.opt}$ (bar)	$\dot{Q}_{o.co2.opt}$ (W)	COP_{opt} (-)	$\dot{W}_{plant.opt}$ (W)	$\Delta\dot{Q}_{o.co2.opt}$ (%)	ΔCOP_{opt} (%)	$\Delta P_{GC\text{-}K.opt}$ (bar)	$\Delta\dot{W}_{plant.opt}$ (%)
Base cycle									
0.2	34.9	86.2	834.2	1.92	433.8	-	-	-	-
0.2	30.1	79.6	930.2	2.33	399.5	-	-	-	-
0.2	25.2	70.2	1039.2	3.01	345.2	-	-	-	-
0.3	20.3	62.2	1183.9	3.82	310.3	-	-	-	-
−9.9	34.7	87.0	571.9	1.39	411.5	-	-	-	-
−9.8	30.0	77.0	646.5	1.69	383.5	-	-	-	-
−9.8	25.1	70.1	705.2	1.98	356.9	-	-	-	-
−9.7	20.0	62.5	791.2	2.42	327.0	-	-	-	-
IHX cycle									
0.1	35.0	85.6	852.7	2.03	421.0	+2.2	+5.3	−0.6	−2.9
0.0	29.9	77.8	970.9	2.43	399.2	+4.4	+4.4	−1.8	−0.1
−9.7	34.6	86.6	604.4	1.48	409.6	+5.7	+6.2	−0.4	−0.5
−9.8	29.9	75.0	651.6	1.75	381.8	+3.3	+3.7	−2.0	−0.4
MS cycle									
0.2	35.1	84.2	1047.1	2.19	478.9	+25.5	+13.7	−2.0	+10.4
0.2	30.0	75.0	1109.8	2.54	436.7	+19.3	+9.2	−4.6	+9.3
0.3	25.1	70.2	1294.2	3.07	421.9	+24.5	+1.9	0	+22.2
0.3	20.0	62.2	1338.1	3.54	377.6	+13.0	−7.1	0	+21.7
−9.8	35.0	84.2	787.2	1.61	488.1	+37.7	+16.1	−2.8	+18.6
−9.8	30.0	75.0	855.6	1.89	451.9	+32.3	+12.3	−2.0	+17.9
−9.9	25.0	70.1	913.4	2.13	428.6	+29.5	+7.9	0	+16.1
−9.9	19.9	62.5	964.8	2.50	386.2	+21.9	+3.3	0	+12.3

According to Table 4 the increment of COP is higher the lower the evaporating level and the higher the heat-rejection temperature become. This trend is similar for cooling capacity, except for one test with mechanical subcooling (25 °C at 0 °C). Regarding optimal pressure, the subcooling process lowered the optimal heat-rejection pressure from 0.4 to 4.6 bar depending on the configuration. This reduction affects positively the stability of the refrigerating plant minimizing the sharpest drop of COP when it operates close to the pseudocritical temperature [52]. Again, it is important to remark that the previous results are obtained from a non-optimized MS cycle.

3.5. Subcooling Effect

The subcooling effect is the difference between the temperature at the gas-cooler/condenser outlet ($T_{GC\text{-}K.out}$) and the temperature at the inlet of the back-pressure valve ($T_{BP.in}$). Figure 7 presents the average values of both temperatures at the two evaporating levels (0 and −10 °C) for each configuration analysed.

Taking into account the presented experimental results, some aspects can be highlighted. The first is that the important subcooling degree reached by using a phase-change fluid (MS system) instead of a cold vapour (IHX system). This effect was due to the greater heat transfer coefficients reached during the evaporation process as well as the higher heat transfer area of the subcooler (almost 10 times the heat transfer area of the IHX).

The second is the higher subcooling effect at low evaporating temperatures regardless of the configuration. In this case, the refrigerant mass flow rate is higher at 0 °C than −10 °C so it reduces the subcooling effect introduced by both configurations.

Finally, the trend of the temperature at the back-pressure inlet ($T_{BP.in}$) changes sharply near the pseudocritical temperature (dotted line). This abrupt change is due to the high values reached by the specific heat near the critical point which main consequence is the reduction of the subcooling effect according to Equation (8). This reduction directly affects the trend of the COP curve depicted in Figure 6 especially at the heat-rejection temperatures of 30 and 35 °C:

$$\dot{Q}_{SUB.CO2} \approx \dot{m}_{CO2} \cdot \overline{c_{P}}_{CO2} \cdot \Delta T_{SUB} \quad (8)$$

Despite the pseudocritical point is far from the optimal pressure at high rejection temperatures, it affects the behaviour of the subcooler and IHX so their designs need to consider similar aspects used in the gas-cooler modelling [23,53].

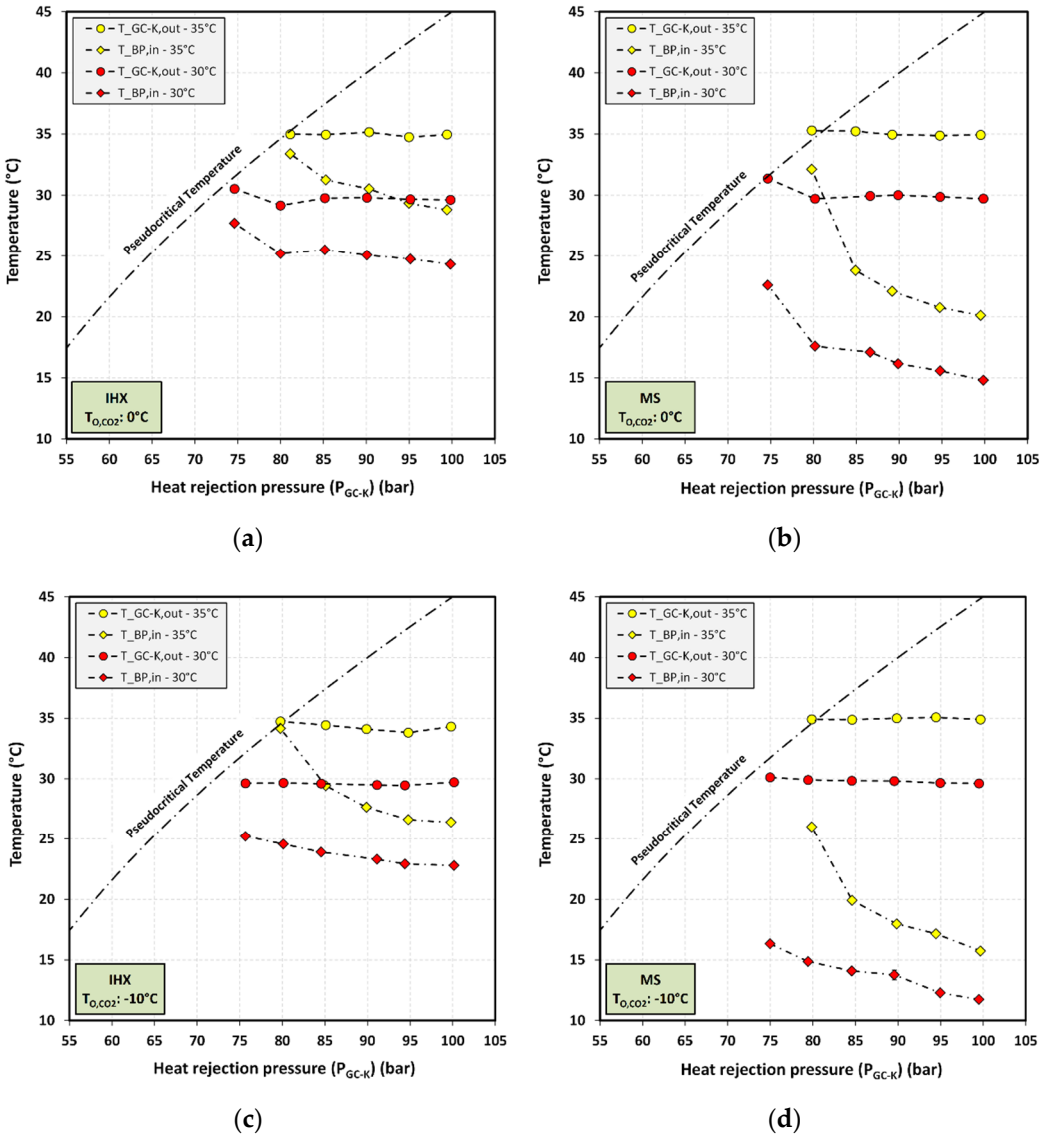

Figure 7. Trends for $T_{BP,in}$ and $T_{GC-K,out}$ with the heat rejection pressure (P_{GC-K}) at 0 °C with IHX (**a**) and MS system (**b**), and at −10 °C with IHX (**c**) and MS system (**d**).

4. Computational Model

4.1. Model Description

The model of the MS system is composed of two interrelated blocks that model the CO_2 transcritical refrigeration cycle and the mechanical subcooling unit. The relation between both blocks is made by the subcooler (6) that acts as an evaporator in the mechanical subcooling cycle and as subcooler in the CO_2 transcritical refrigeration cycle. In each block, it has been assumed no pressure drops along pipelines and heat exchangers, as well as no heat transfer to the ambient. The unique pipeline where heat exchange has been assumed is the suction line, where constant superheating has been taken into account in both cycles. Regarding the expansion devices, all have been assumed as adiabatic.

4.1.1. Transcritical Cycle Model

The transcritical model is equipped with a double-stage throttling expansion similar to Figure 1. This arrangement controls simultaneously the optimal heat rejection pressure and the useful superheating at the evaporator (SH_{CO2}). The model assumes a constant value for the evaporating temperature ($T_{O.CO2}$) and the temperature at the exit of the evaporator ($T_{O.CO2.out}$) is calculated with Equation (9):

$$T_{O.CO2.out} = T_{O.CO2} + SH_{CO2} \quad (9)$$

The gas-cooler/condenser outlet temperature ($T_{GC\text{-}K.out}$) is obtained from Equation (10) by adding an approach temperature (ΔT_{GC-K}) to the heat rejection temperature ($T_{W.in}$). The value of this approach temperature depends on the working conditions of the refrigerating facility. Thus, in transcritical conditions, an approach temperature of 0.5 K has been obtained from the experimental tests while a value of 1.5 K has been registered working in subcritical conditions:

$$T_{GC-K.out} = T_{W,in} + \Delta T_{GC-K} \quad (10)$$

Regarding the heat rejection pressure (P_{GC-K}), its value can be fixed from 110 bar to a minimum pressure defined by the gas-cooler/condenser outlet temperature ($T_{GC\text{-}K.out}$). The criterion is as follows: if $T_{GC\text{-}K.out} \geq 31$ °C the model is assumed that operates under transcritical conditions and the minimum pressure is defined by the gas-cooler outlet temperature (Equation (9)) and the specific enthalpy in the critical point (approx. 326.1 kJ·kg^{-1}). This minimum pressure guarantees the stability of the refrigerating plant because fix the pressure of the liquid receiver below the critical one (73.8 bar). On the other hand, if $T_{GC\text{-}K.out} < 31$ °C a subcritical operation is possible, so the minimum pressure would correspond to the condensing pressure at the temperature defined by Equation (9). In this case, it should be noted that the operation with a mechanical subcooling system needs to by-pass the liquid receiver to reduce the maximum pressure.

The operation of the compressor is defined by Equations (11) and (12), that determine the refrigerant mass flow rate ($\dot{m}$) and the electrical power consumption ($\dot{W}_C$):

$$\dot{m} = \frac{\eta_V \cdot V_g \cdot \frac{N}{60}}{v_{C,in}} \quad (11)$$

$$\dot{W}c = \dot{m} \cdot \frac{(h_{C,out,iso} - h_{C,in})}{\eta_G} \quad (12)$$

The global efficiency (η_G) and volumetric efficiency (η_V) have been adjusted by the least-square best-fit method using the experimental data and the equations published by Sánchez et al. [54]. Equations (13) and (14) present both parameters depending on the suction pressure ($P_{C,in}$), the discharge pressure ($P_{C,out} = P_{GC-K}$) and the temperature at the suction port ($T_{C,in}$). This last is defined by Equation (15) as the sum of the temperature at the exit of the evaporator ($T_{O.CO2.out}$) and the superheating in the suction line (SH_{SL}). Table 5 summarises the coefficients of these equations, including the maximum deviation (ε_{max}), and the validity range;

$$\eta_V = a_0 + a_1 \cdot P_{C,in} + a_2 \cdot P_{C,out} + a_3 \cdot T_{C,in} \quad (13)$$

$$\eta_G = a_0 + a_1 \cdot P_{C,in} + a_2 \cdot P_{C,out} + a_3 \cdot T_{C,in} \quad (14)$$

$$T_{C.in} = T_{O.CO2.out} + SH_{SL} \quad (15)$$

Finally, the cooling capacity of the CO_2 transcritical cycle ($\dot{Q}_{O.CO2}$) is defined by Equation (1) where the specific enthalpy at the evaporator inlet ($h_{O,CO2,in}$) is assumed equal to the specific enthalpy at the back-pressure inlet ($h_{BP,in}$). This enthalpy depends on the subcooling degree introduced by the mechanical subcooling system.

Table 5. Experimental coefficients for the CO_2 hermetic compressor.

R744 Compressor				
Coefficient	η_V	η_G	**Parameter**	**Validity Range**
a_0	0.8544215784	0.5257504376	$P_{C,i}$ (bar)	35.52 ÷ 26.04 bar
a_1	0.0041278179	−0.0008023276	$T_{C,i}$ (°C)	19.90 ÷ −5.36 °C
a_2	−0.0030962470	−0.0000199178	$P_{C,o}$ (bar)	100.30 ÷ 62.14 bar
a_3	0.0019119523	0.0017955538	η_V	0.82 ÷ 0.63
ε_{max}	7.95%	7.59%	η_G	0.55 ÷ 0.47

4.1.2. Mechanical Subcooling Model

The mechanical subcooling unit is single-stage vapour compression cycle connected to the transcritical one by means of the subcooler. To model this last, two parameters have been taken into account: the subcooling degree in the CO_2 transcritical cycle (ΔT_{SUB}) and the thermal effectiveness of the subcooler (ε_{SUB}). The subcooling allows determining the temperature at the inlet of the back-pressure ($T_{BP,in}$) with Equation (16). It is a key parameter to optimize the performance of the refrigerating plant so it can be either fixed externally for sizing the compressor of the mechanical subcooling unit, or calculated if the capacity of the compressor is known:

$$T_{BP,in} = T_{GC-K.out} - \Delta T_{SUB} \tag{16}$$

Regarding the thermal effectiveness of the subcooler (ε_{SUB}), from experimental tests, the resulting thermal effectiveness is ranged from 82.8 to 98.7% depending on the operating conditions. The model assumes a constant value of 85% taking CO_2 as the fluid with less thermal capacity. Using Equation (17), the evaporating level of the mechanical subcooling system ($T_{O.MS}$) can be obtained:

$$T_{O.MS} = T_{GC-K.out} - \frac{\Delta T_{SUB}}{\varepsilon_{SUB}} \tag{17}$$

The temperature at the exit of the subcooler ($T_{O.MS.out}$) is determined by adding useful superheating (SH_{MS}) as shown in Equation (18):

$$T_{O.MS.out} = T_{O.MS} - SH_{MS} \tag{18}$$

The condensing temperature of the mechanical subcooling cycle ($T_{K.MS}$) can be determined by Equation (19) assuming a constant temperature approach ($\Delta T_{K.MS}$) concerning the heat-rejection temperature ($T_{W.in}$). From experimental tests this value has an average value of 0.5 K due to the important heat transfer area of the condenser:

$$T_{K.MS.out} = T_{W.in} - \Delta T_{K.MS} \tag{19}$$

The temperature at the exit of the condenser ($T_{K.MS.out}$) is obtained with Equation (20) assuming a fixed subcooling at the condenser ($SUB_{K.MS}$). From the experimental tests this value is almost constant and has a value of 2 K:

$$T_{K.MS} = T_{K.MS.out} - SUB_{K.MS} \tag{20}$$

Similarly to the model of the CO_2 compressor, the compressor of the mechanical subcooling system has been modelled with the Expressions 13 to 15 using the experimental data. Table 6 shows the adjusted coefficients including the maximum deviation (ε_{max}), and the validity range.

Table 6. Experimental coefficients for the R600a hermetic compressor.

R600a Compressor				
Coefficient	η_V	η_G	**Parameter**	**Validity Range**
a_0	1.0892397842	0.1416032159	$P_{C,in}$ (bar)	3.94 ÷ 2.11 bar
a_1	−0.1479503029	−0.1381438733	$T_{C,in}$ (°C)	34.56 ÷ 11.10 °C
a_2	−0.0389382148	0.0810000150	$P_{C,out}$ (bar)	5.00 ÷ 3.57 bar
a_3	0.0175038421	0.0048250042	η_V	0.85 ÷ 0.79
ε_{max}	5.53%	10.06%	η_G	0.40 ÷ 0.21

4.1.3. Refrigerating Plant

Once both models are described, the overall COP of the refrigerating plant is defined with Equation (7). The optimization of the COP through the heat rejection pressure (P_{GC-K}) and the subcooling degree (ΔT_{SUB}) will be described in Section 5.

4.2. Model Validation

To validate the results from the model, Section 4.2 includes a comparison between the experimental results from tests and the results calculated using the model. The variables that have been used as input data of the computational model are heat rejection pressure (P_{GC-K}), heat rejection temperature ($T_{W.in}$), the evaporating temperature of the CO_2 cycle ($T_{O.CO2}$) and cubic capacity of both compressors ($V_{g.CO2}$ $V_{g.CO2}$). The variables set with a constant value are temperature approach in the gas-cooler (ΔT_{GC}): 0.5 K/1.5 K, subcooling in the condenser of the MS cycle ($SUB_{K.MS}$): 2 K, temperature approach in the condenser of the MS cycle ($\Delta T_{K.MS}$): 0.5 K, subcooler thermal effectiveness (ε_{SUB}): 85%, suction line superheating (SH_{SL}): 5 K, and useful superheating in both cycles (SH_{MS} and SH_{CO2}): 3.5 K.

Figure 8 compares the experimental and the theoretical results for the parameters of COP and cooling capacity. As it can be shown there is a good agreement between the averaged experimental data and the results from the computational model. In terms of cooling capacity, more than 91% of data have a deviation of ≤6%, while for COP, more than 83% of data have a deviation of ≤6%. Therefore, we can affirm that the developed model can be adopted as a reliable one.

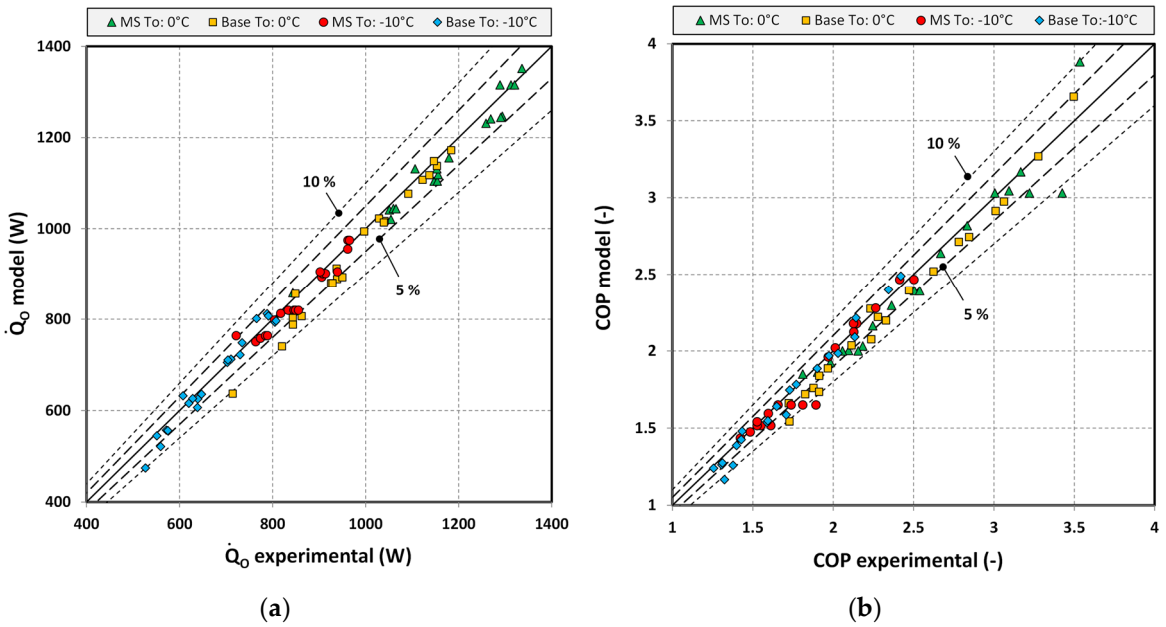

(**a**) (**b**)

Figure 8. Validation of the computational model using the cooling capacity (**a**) and the COP of the refrigerating plant (**b**) with experimental data.

5. Optimization Analysis

5.1. Model Operation

With the aid of the computational model described before, the COP of the refrigerating plant can be maximized not only identifying the optimal heat rejection pressure ($P_{GC-K,opt}$) but also determining the optimum subcooling degree ($\Delta T_{SUB,opt}$). This double optimization allows sizing the mechanical subcooling compressor at each operating conditions which are very useful to control the compressor rotation speed if it is possible. Table 7 summarizes the input data of the model including those variables assumed as constant in the model operation.

Table 7. Input data values to the computation model.

Variable	Description	Value/Range
$T_{O.CO2}$ (°C)	Evaporation level	−10 °C
$SH_{CO2}SH_{MS}$ (K)	Useful superheating in CO_2 and MS cycle	3.5 K
SH_{SL} (K)	Superheating in suction line	5 K
$T_{W.in}$	Heat rejection temperature	20 ÷ 40 °C
P_{GC-K}	Heat rejection pressure	110 ÷ P_{min} bar
ΔT_{GC-K}	Approach temperature in the gas-cooler/condenser	0.5 K/1.5 K
ΔT_{SUB}	Subcooling degree	2 ÷ 30 °C
ε_{SUB}	Subcooler thermal effectiveness	85%
$\Delta T_{K.MS}$	Approach temperature in the condenser of MS cycle	0.5 K
$SUB_{K.MS}$	Subcooling in the condenser of MS cycle	2 K
N	Compressor rotation speed	2900 rpm
$V_{g.CO2}$	CO_2 compressor cubic capacity	1.75 cm^3

At each heat rejection temperature, the gas-cooler/condenser pressure has varied from 110 bar to the minimum (P_{min}) defined by the gas-cooler/condenser outlet temperature ($T_{GC-K.out}$). Similarly, the subcooling degree has also modified from 2 to 30 K at each heat rejection pressure. As a result, the computational model gives a COP matrix where the maximum is determined and the optimized variables are defined.

5.2. Mechanical Subcooling Refrigerants

Maintaining the conditions described in Table 7, the computational model has been used to evaluate five low-GWP refrigerants potentially used in commercial refrigeration and allowed by the European Regulation EU No 517/2014: R600a, R290, R152a and R1234yf. Table 8 summarizes the main thermodynamic properties of these refrigerants. Table 8 also includes the ASHRAE classification [55] and the $GWP_{100\ years}$ values [56].

Table 8. Thermodynamic properties, safety classification and GWP values for the analyzed refrigerants.

Fluid	Family	P_{crit} (bar)	T_{crit} (bar)	MW ($kg \cdot kmol^{-1}$)	NBP (°C)	v_C (10 °C) ($m^3 \cdot kg^{-1}$)	λ (10 °C) ($kJ \cdot kg^{-1}$)	q_v (10 °C) ($kJ \cdot m^{-3}$)	Safety Group	GWP (100 Years)
R152a	HFC	45.2	113.3	66.1	−24.0	0.0858	296.6	3455.6	A2	137
R1234yf	HFO	33.8	94.7	114.0	−29.5	0.0412	156.6	3800.2	A2L	<1
R600a	HC	36.3	134.7	58.1	−11.8	0.1704	344.6	2022.0	A3	4
R290	HC	42.5	96.7	44.1	−42.1	0.0726	360.3	4965.5	A3	3

To best fit the model with each refrigerant, Table 9 shows the adjusted coefficients for the mechanical subcooling compressor excepting R600a which coefficients are summarized in Table 6. These values have been determined from the experimental results published by Sánchez et al. [57].

Table 9. Experimental coefficients for the hermetic compressors.

Coefficient	η_V	η_G	Parameter	Validity Range
R290 Compressor				
a_0	0.8245644392	0.3753611180	$P_{C,in}$ (bar)	5.47 ÷ 3.40 bar
a_1	0.0177395862	−0.0289761062	$T_{C,in}$ (°C)	24.29 ÷ −2.01 °C
a_2	−0.0112283110	0.0129968640	$P_{C,out}$ (bar)	15.40 ÷ 9.57 bar
a_3	0.0017747630	0.0010797776	η_V	0.84 ÷ 0.71
ε_{max}	1.37%	8.38%	η_G	0.47 ÷ 0.33
R152a Compressor				
a_0	0.7566171921	0.2754222011	$P_{C,in}$ (bar)	3.72 ÷ 1.74 bar
a_1	0.0273964137	−0.0434225620	$T_{C,in}$ (°C)	28.59 ÷ 10.17 °C
a_2	−0.0142596520	0.0227531186	$P_{C,out}$ (bar)	10.44 ÷ 5.94 bar
a_3	0.0019095772	0.0013423916	η_V	0.80 ÷ 0.67
ε_{max}	2.48%	17.54%	η_G	0.44 ÷ 0.24
R1234yf Compressor				
a_0	0.7397796396	0.2540133488	$P_{C,in}$ (bar)	4.27 ÷ 2.10 bar
a_1	0.0110698197	−0.0518935273	$T_{C,in}$ (°C)	27.38 ÷ 5.69 °C
a_2	−0.0090766299	0.0231816838	$P_{C,out}$ (bar)	11.75 ÷ 6.84 bar
a_3	0.0022774913	0.0021953016	η_V	0.76 ÷ 0.66
ε_{max}	3.74%	13.64%	η_G	0.43 ÷ 0.21

5.3. Model Results

Table 10 gathers the results from the model using the refrigerants presented in Section 5.3. All data is presented at the optimal operating conditions. The parameters included in Table 10 are the optimal heat-rejection pressure ($P_{GC\text{-}K.opt}$), the optimal subcooling degree ($\Delta T_{SUB.opt}$), the cooling capacity ($\dot{Q}_{O.CO2.opt}$), the power consumption of the refrigerating plant ($\dot{W}_{plant.opt}$), the optimum COP of the facility (COP_{opt}), the displacement of the mechanical subcooling compressor ($V_{g.MS}$) and its corresponding compression ratio (t_{MS}). Last columns show the variation of the parameters stated above taking the Base cycle as a reference. Equations (21) and (22) allow determining these increments with "X" as the variable analysed:

$$\Delta X = 100 \cdot \frac{X_{MS} - X_{Base}}{X_{Base}} \quad (21)$$

$$\Delta P_{GC-K} = P_{GC-K,opt\ MS} - P_{GC-K,opt\ Base} \quad (22)$$

Table 10. Results at the optimal operating conditions.

$T_{W.in}$ (°C)	$P_{GC\text{-}K.opt}$ (bar)	$\dot{Q}_{o.co2.opt}$ (W)	$\dot{W}_{plant.opt}$ (W)	COP_{opt} (-)	$\Delta T_{SUB.opt}$ (K)	$\dot{V}_{g.MS}$ (cm^3)	t_{MS} (-)	$\Delta\dot{Q}_O$ (%)	$\Delta\dot{W}_{plant}$ (%)	ΔCOP (%)	ΔP_{GC-K} (bar)
Base cycle											
40	105.73	469.1	459.5	1.02	-	-	-	-	-	-	-
36	93.74	519.7	437.6	1.19	-	-	-	-	-	-	-
32	82.27	574.3	406.8	1.41	-	-	-	-	-	-	-
28	73.90	618.5	377.0	1.64	-	-	-	-	-	-	-
24	65.09	697.9	337.7	2.07	-	-	-	-	-	-	-
20	59.34	784.1	306.8	2.56	-	-	-	-	-	-	-
MS cycle using R152a											
40	94.75	761.4	554.6	1.37	22.78	2.88	2.31	62.3%	20.7%	34.5%	−10.98
36	86.85	788.4	514.4	1.53	19.18	2.48	2.06	51.7%	17.5%	29.1%	−6.89
32	78.40	817.7	467.2	1.75	15.70	2.10	1.84	42.4%	14.9%	23.9%	−3.87
28	71.65	842.2	424.2	1.99	13.26	1.83	1.65	36.2%	12.5%	21.0%	−2.25
24	65.09	887.4	376.5	2.36	11.54	1.45	1.57	27.1%	11.5%	14.0%	0.00
20	59.34	930.6	333.3	2.79	9.74	1.16	1.48	18.7%	8.6%	9.3%	0.00
MS cycle using R1234yf											
40	96.10	731.1	562.5	1.30	20.12	2.46	2.10	55.9%	22.4%	27.3%	−9.63
36	87.70	759.0	520.5	1.46	16.64	2.08	1.88	46.0%	18.9%	22.8%	−6.04
32	78.85	787.2	470.4	1.67	13.18	1.71	1.68	37.1%	15.6%	18.5%	−3.42
28	71.85	809.6	424.3	1.91	10.68	1.44	1.50	30.9%	12.5%	16.3%	−2.05
24	65.09	854.1	373.5	2.29	8.92	1.08	1.42	22.4%	10.6%	10.6%	0.00
20	59.34	899.9	329.7	2.73	7.34	0.83	1.35	14.8%	7.5%	6.8%	0.00
MS cycle using R600a											
40	95.30	734.7	551.8	1.33	20.26	3.80	2.08	56.6%	20.1%	30.4%	−10.43
36	87.25	759.5	511.6	1.48	16.58	3.20	1.85	46.1%	16.9%	25.0%	−6.49
32	78.60	785.7	463.8	1.69	13.00	2.63	1.65	36.8%	14.0%	20.0%	−3.67
28	71.75	807.5	419.8	1.92	10.50	2.22	1.48	30.5%	11.4%	17.2%	−2.15
24	65.09	851.4	371.3	2.29	8.72	1.66	1.40	22.0%	10.0%	10.9%	0.00
20	59.34	895.9	328.4	2.73	7.04	1.26	1.33	14.3%	7.0%	6.8%	0.00
MS cycle using R290											
40	94.35	764.7	549.2	1.39	23.00	2.07	2.07	63.0%	19.5%	36.4%	−11.38
36	86.55	797.2	510.8	1.56	19.94	1.84	1.91	53.4%	16.7%	31.4%	−7.19
32	78.25	831.9	465.8	1.79	16.94	1.61	1.76	44.9%	14.5%	26.5%	−4.02
28	71.60	852.1	423.1	2.01	14.08	1.40	1.63	37.8%	12.2%	22.8%	−2.30
24	65.09	900.9	377.2	2.39	12.66	1.13	1.57	29.1%	11.7%	15.6%	0.00
20	59.34	946.0	334.7	2.83	11.00	0.92	1.50	20.6%	9.1%	10.6%	0.00

5.3.1. Optimal Subcooling Degree

Figure 9 presents the optimal subcooling degree generated by the mechanical subcooling unit at different heat rejection temperatures. As it can be shown, the subcooling rises as the heat rejection temperature is higher regardless of the refrigerant used. However, refrigerants R152a and R290 need higher subcooling degrees to reach the optimal performance in contrast with R600a and R1234yf, which values are on average 2.7 to 3.6 K lower. Similar trends were obtained by Dai et al. [41] using R152a as a refrigerant.

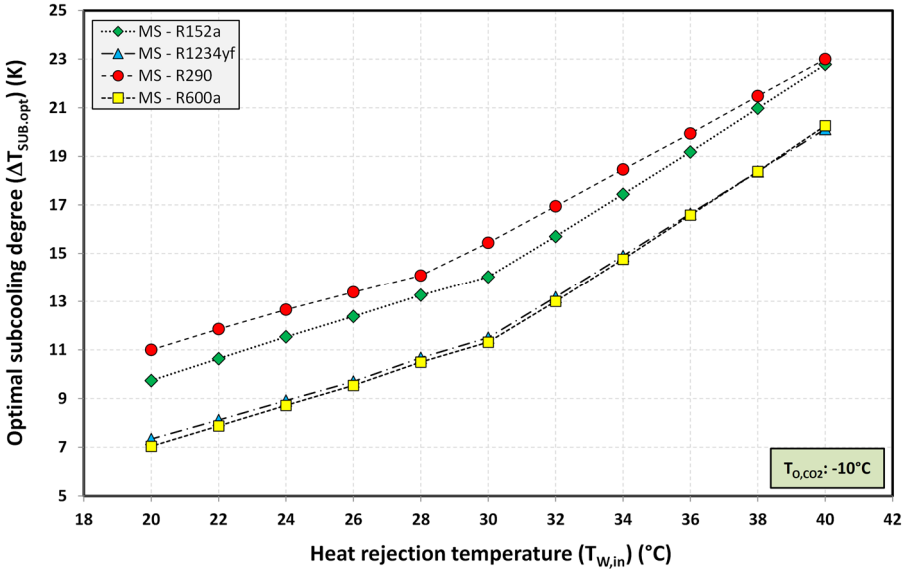

Figure 9. Optimum subcooling degree at different heat rejection temperatures.

5.3.2. Optimal Heat Rejection Pressure

As was analyzed experimentally in Table 4, the use of the mechanical subcooling system always reduces the optimal heat rejection pressure of the refrigerating plant. Figure 10 supports those results with a clear reduction of the optimal heat pressure as the heat rejection temperature rises. Moreover, it is noticed that the influence of the mechanical subcooling refrigerants in the optimal pressure is negligible.

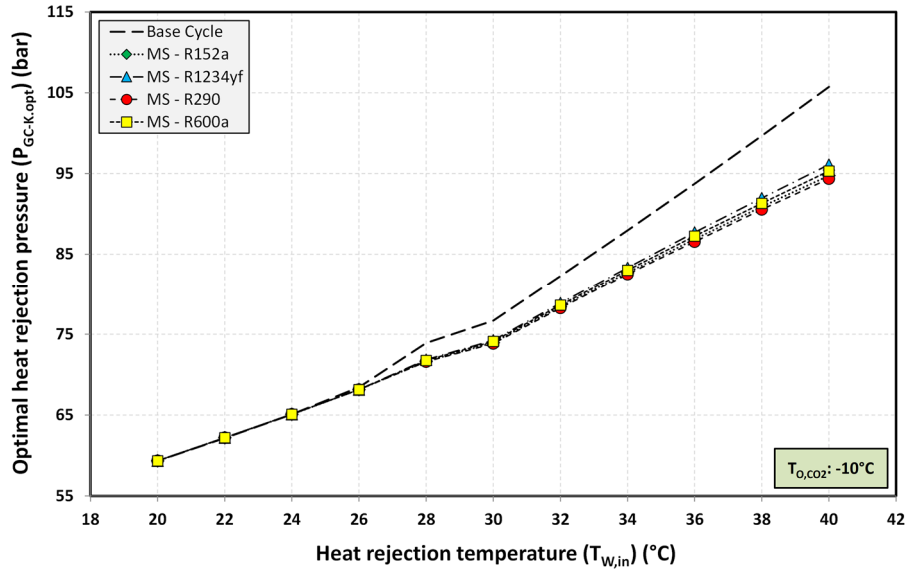

Figure 10. Optimum heat rejection pressure at different heat rejection temperatures.

5.3.3. Cooling Capacity

The cooling capacity impact of implementing a mechanical subcooling system is presented in Figure 11. Regarding the Base cycle, the presence of the subcooling system always rises the cooling capacity with a positive trend regarding the heat rejection temperature. This trend is in agreement with the experimental results summarized in Table 4, where the effects are lower because the refrigerating plant is not working at the optimal conditions.

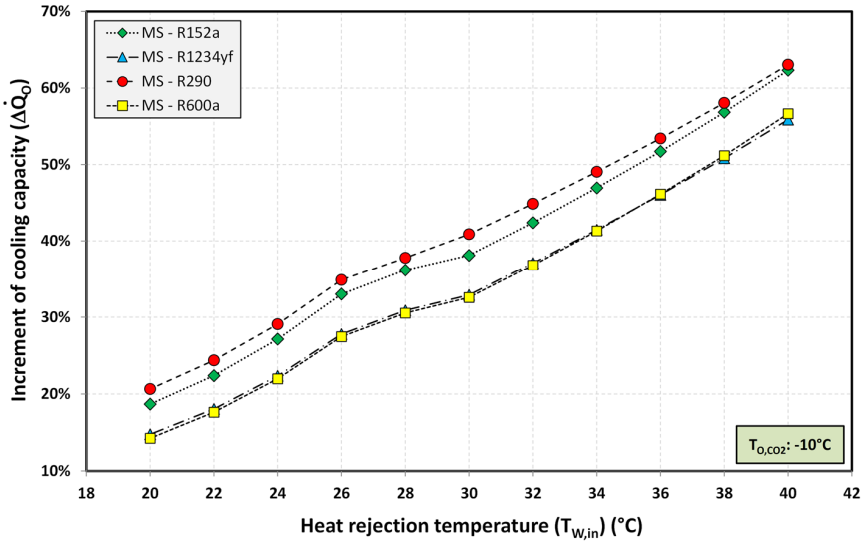

Figure 11. Increment of cooling capacity at the optimal operating conditions vs. heat rejection pressure.

According to Figure 11, the use of R290 and R152a in the mechanical subcooling unit performs better than R600a or R1234yf, which effects are quite similar.

5.3.4. Power Consumption

As a result of adding a refrigerating cycle to reduce the temperature at the exit of the gas-cooler, the power consumption of the refrigerating plant increases as well as its complexity. This increment depends on the heat rejection temperature and the refrigerant used in the mechanical subcooling unit as it showed Figure 12.

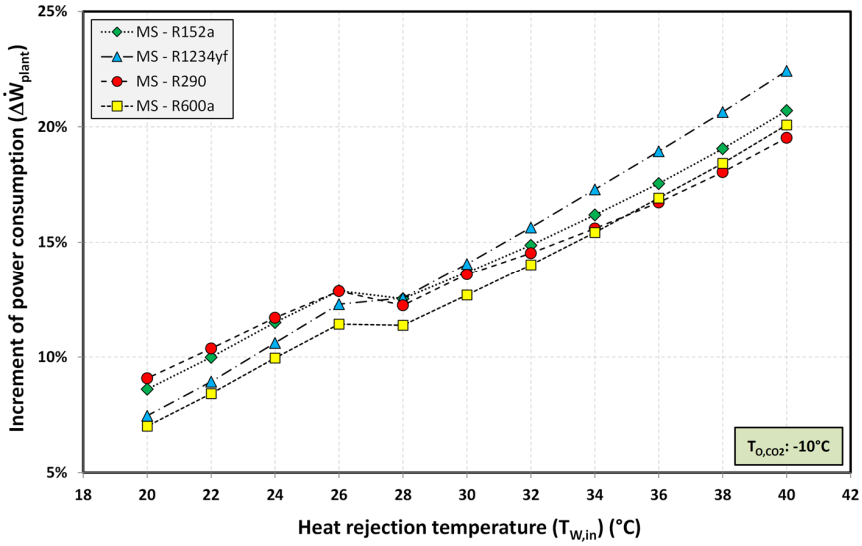

Figure 12. Increment of power consumption at the optimal operating conditions vs. heat rejection pressure.

From Figure 12 is evident that the increment in power consumption is higher as higher the heat rejection temperature is. Moreover, the use of R600a reduces the power consumption in almost all analyzed temperature range.

5.3.5. COP

The COP of the modified refrigerating plant is depicted in Figure 13 as a function of the heat rejection temperature and the refrigerants used in the auxiliary system.

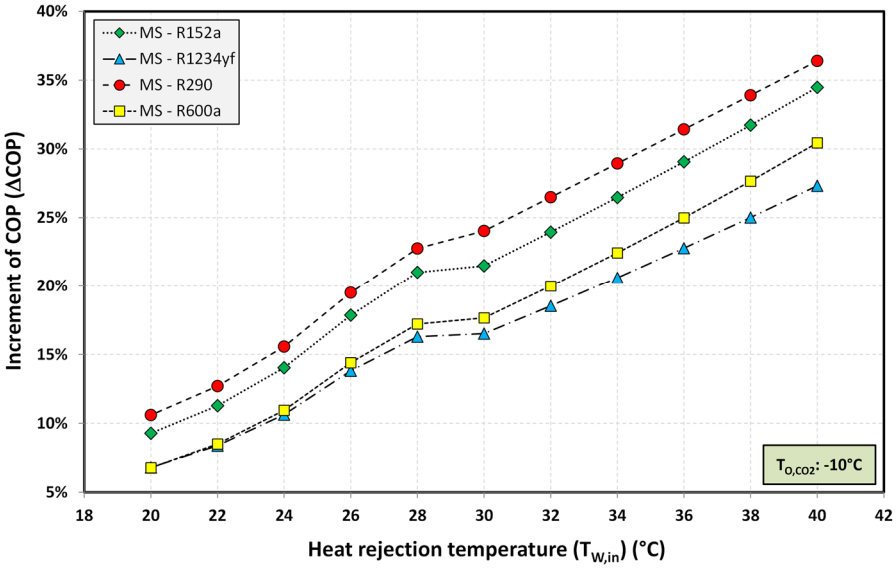

Figure 13. Increment of COP at the optimal operating conditions vs. heat rejection pressure.

As Figure 13 show, at the optimal operating conditions, the effect of the mechanical subcooling is always positive especially at high values of heat rejection temperatures. This positive effect depends on the refrigerant used in the auxiliary system where the R290 and R152a are the best options among the fluids analyzed in this work. In percentage terms, the increment of COP by using R290 is ranged between 10.6 and 36.4% while R152a yields in a range from 9.3 to 34.5% at the same heat rejection temperatures. The refrigerant R600a experimentally tested in this work increases the COP from 6.8 to 30.4%, which is better than the HFO R1234yf which results varied from 6.8 to 27.3%. On the other hand, at low heat rejection temperatures, the refrigerants R152a and R290 report values of compression ratio (t_{MS}) higher than the reported by R600a or R1234yf. This is particularly important in ensuring the lifetime of the compressor according to the compressor's manufacturers [58].

5.3.6. Compressor Capacity Ratio

The compressor capacity ratio (VR) calculated with Equation (23) is defined as the ratio between the cubic capacity of the CO_2 compressor and the cubic capacity of the mechanical subcooling compressor. This adimensional parameter gives information about the optimal design of the subcooling compressor concerning the CO_2 compressor. Figure 14 graphically presents VR for each refrigerant analyzed:

$$VR = \frac{V_{CO2}}{V_{MS}} \tag{23}$$

Considering the information depicted in Figure 14, two important points can be highlighted. The first one, the cubic capacity of the subcooling compressor increases as higher is the heat rejection temperature. This trend is in accordance with the required subcooling degree to reach the optimum conditions showed in Figure 7. The second one, the VR ratio depends to a great extent on the refrigerant used in the subcooling system. Thus, the use of refrigerants with a low specific volume at the suction

conditions results in small compressors with a cubic capacity similar o lower than the CO_2 one. This is the case of R290 and R1234yf which values of VR are higher than R152a and R600a.

The experimental plant analyzed in this work has a VR equal to 0.643 which corresponds to the optimal design for the heat rejection temperature of 32.7 °C.

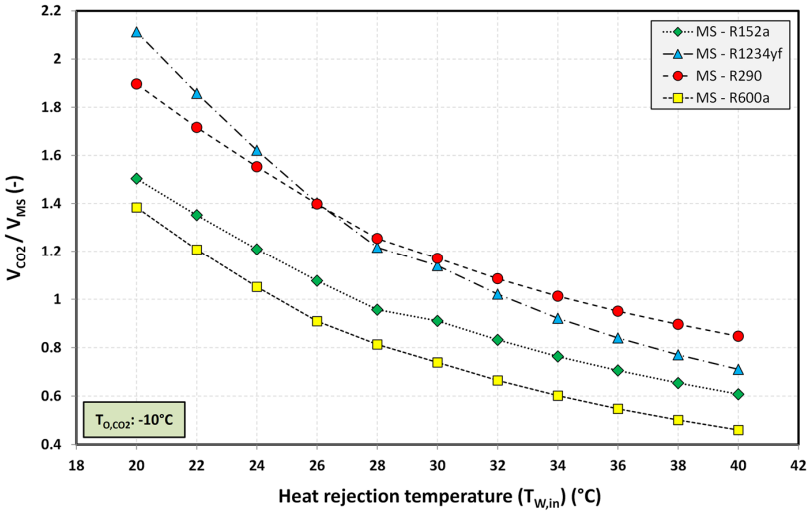

Figure 14. Compressor capacity ratio at the optimal operating conditions vs. heat rejection pressure.

6. Conclusions

This extensive work analyzes and optimizes the operation of a CO_2 refrigeration plant upgraded with a mechanical subcooling unit using different refrigerants. To achieve this target, the work presents an experimental analysis where the effect of using an R600a mechanical subcooling unit is discussed and compared with the use of a suction-to-liquid heat exchanger (IHX). From this experimental approach, the following conclusions were obtained at the optimum operating point (maximum COP):

- The electrical power consumption of the whole refrigerating plant is hardly affected by the IHX but significantly modified by the mechanical subcooling system. The increment registered with the mechanical subcooling arrangement is rated between 9.3 and 22.2%.
- The cooling capacity of the refrigerating facility rises with the heat rejection temperature regardless of the subcooling system installed. Thus, the presence of the IHX allows increments up to 5.7% while the use of the mechanical subcooling system performs better results up to 37.7%.
- The combined effect of both parameters are defined by the COP. Concerning the Base cycle, the use of the IHX reports an increment up to 6.2% while the installation of a mechanical subcooling unit results in a maximum increment of 16.1%.
- Finally, the optimal heat rejection pressure decreases in both arrangements: up to 2 bar with the IHX and up to 4.6 bar using the mechanical subcooling unit.

Taking into account the experimental data, a computational model of the whole refrigerating system was developed and validated with a deviation lower than 6% in terms of COP and cooling capacity. The model was used to optimize the whole refrigerating plant taking the heat rejection pressure and the subcooling degree as key parameters at different heat rejection temperatures.

To quantify the effect of using different refrigerants in the mechanical subcooling unit, four refrigerants where analyzed and compared with the computational model: R600a, R290, R152a and R1234yf. From this analysis at the optimum operating conditions, the following conclusions were obtained fixing the capacity of the R744 compressor:

- The optimal subcooling degree that maximizes the COP of the refrigerating plant rises as the heat rejection temperature is higher. Moreover, this subcooling degree is higher for the refrigerants R152a and R290, and quite similar for the refrigerants R1234yf and R600a.

- The optimal heat rejection pressure lowers with the presence of the mechanical subcooling system. This reduction is higher as higher the heat rejection temperature is, and it is hardly affected by the refrigerant used in the mechanical subcooling unit.
- The positive effect on the cooling capacity is always higher at high heat rejection temperature. It depends on the refrigerant used and it is always higher for the refrigerants R290 and R152a.
- The power consumption rises with the heat rejection temperature due to the presence of an auxiliary cycle which power consumption depends on the refrigerant used. For low heat rejection temperatures (20–26 °C), the R600a and the R1234yf report the lower increment of power while at high rejection temperatures (36–40 °C) the most suitable are R290 and R600a.
- Concerning the COP of the refrigerating plant, the results from the computational model reveal that R290 is the best option for the mechanical subcooling unit followed by the R152a, R600a and R1234yf. The increment calculated with propane ranges from 10.6% at 20 °C to 36.4% at 40 °C, while the improvements with R152a falls within a range from 9.3% at 20 °C and 34.5% at 40 °C.
- Finally, the compressor capacity ratio at the optimal conditions shows that the use of the R290 in the mechanical subcooling unit ensures the most compact system among the other refrigerants for heat rejection temperatures higher than 26 °C. In terms of security, this helps to reduce the mass charge of the flammable refrigerant in the auxiliary system.

Author Contributions: Investigation, D.S., J.C.-G., R.C. and R.L.; Methodology, D.S. and J.C.-G.; Project administration, R.C.; Validation, R.L.; Writing—original draft, D.S.; Writing—review & editing, D.C.-A. and L.N.-A. All authors have read and agreed to the published version of the manuscript.

Funding: This research was funded by the Ministerio de Ciencia y Tecnología (Spain) with the project RTI2018-093501-B-C21, and the Jaume I University with the project UJI-B2019-56

Acknowledgments: The authors gratefully acknowledge the Ministerio de Ciencia y Tecnología (Spain) with the project RTI2018-093501-B-C21, and the Jaume I University (Spain) with the project UJI-B2019-56, for financing tis research work.

Conflicts of Interest: The authors declare no conflict of interest. The funders had no role in the design of the study; in the collection, analyses, or interpretation of data; in the writing of the manuscript, or in the decision to publish the results.

Nomenclature

COP	coefficient of performance
DAQ	Data Acquisition System
c_p	specific isobaric heat ($kJ \cdot kg^{-1} \cdot °C^{-1}$)
GWP	Global Warming Potential
h	enthalpy ($kJ \cdot kg^{-1}$)
HFC	hydrofluorocarbon
HFO	hydrofluoroolefin
IHX	suction-to-liquid heat exchanger
$\dot{m}$	mass flow rate ($kg \cdot s^{-1}$)
MS	Mechanical Subcooling system/cycle
N	compressor rotation speed (rpm)
NBP	Normal Boiling Point
P	pressure (bar)
$\dot{q}$	volumetric flow rate ($m^3 \cdot h^{-1}$)
q	volumetric capacity ($kJ \cdot m^{-3}$)
$\dot{Q}$	heat transfer (W)
SH	useful superheating at the evaporator (K)
SUB	subcooling at the exit of condenser (K)
t	pressure ratio
T	temperature (°C)
v	specific volume at the suction port ($m^3 \cdot kg^{-1}$)
V_g	compressor cubic capacity (cm^3)
$\dot{W}$	electrical power consumption (W)

Greek symbols

Δ	increment
ε	thermal effectiveness/error
λ	latent heat ($kJ \cdot kg^{-1}$)
ρ	density ($kg \cdot m^{-3}$)
η_v	volumetric efficiency
η_G	global efficiency

Subscripts

BP	back pressure
C	compressor
CO_2	carbon dioxide; it refers to the carbon dioxide cycle (main cycle)
crit	it refers to the critical point
GC-K	gas-cooler/condenser
Glyc	propylene-glycol mixture (70/30% by mass)
in	inlet
iso	isentropic
K	condenser
max	maximum
min	minimum
MS	it refers to the mechanical subcooling cycle (auxiliary unit)
O	evaporator
opt	optimal
out	outlet
plant	refrigerating plant
R600a	isobutene; it refers to the mechanical subcooling cycle (auxiliary unit)
SL	suction line
SUB	subcooler/subcooling
W	water

References

1. Lorentzen, G. Revival of carbon dioxide as a refrigerant. *Int. J. Refrig.* **1994**, *17*, 292–301. [CrossRef]
2. Robinson, D.M.; Groll, E.A. Efficiencies of transcritical CO_2 cycles with and without an expansion turbine. *Int. J. Refrig.* **1998**, *21*, 577–589. [CrossRef]
3. Finckh, O.; Schrey, R.; Wozny, M. Energy and efficiency comparison between standardized HFC and CO_2 transcritical systems for supermarket applications. In Proceedings of the 23rd IIR International Congress of Refrigeration, Prague, Czech Republic, 21–26 August 2011.
4. Sawalha, S.; Piscopiello, S.; Karampour, M.; Manickam, L.; Rogstam, J. Field measurements of supermarket refrigeration systems. Part II: Analysis of HFC refrigeration systems and comparison to CO_2 trans-critical. *Appl. Therm. Eng.* **2017**, *111*, 170–182. [CrossRef]
5. Karampour, M.; Sawalha, S. Energy efficiency evaluation of integrated CO_2 trans-critical system in supermarkets: A field measurements and modelling analysis. *Int. J. Refrig.* **2017**, *82*, 470–486. [CrossRef]
6. Hafner, A.; Poppi, S.; Nekså, P.; Minetto, S.; Eikevik, T.M. Development of commercial refrigeration systems with heat recovery for supermarket building. In Proceedings of the 10th IIR Gustav Lorentzen Conference on Natural Refrigerants, Delft, The Netherlands, 25–27 June 2012.
7. Polzot, A.; D'Agaro, P.; Cortella, G. Energy Analysis of a Transcritical CO_2 Supermarket Refrigeration System with Heat Recovery. *Energy Procedia* **2017**, *111*, 648–657. [CrossRef]
8. Shecco. F-Gas Regulation Shaking Up the HVAC&R Industry. 2016. Available online: http://publication.shecco.com/publications/view/f-gas-regulation-shaking-up-the-hvac-amp-r-industry (accessed on 19 June 2020).
9. Tsamos, K.M.; Ge, Y.T.; Santosa, I.; Tassou, S.A.; Bianchi, G.; Mylona, Z. Energy analysis of alternative CO_2 refrigeration system configurations for retail food applications in moderate and warm climates. *Energy Convers. Manag.* **2017**, *150*, 822–829. [CrossRef]
10. Gullo, P.; Hafner, A.; Banasiak, K. Transcritical R744 refrigeration systems for supermarket applications: Current status and future perspectives. *Int. J. Refrig.* **2018**, *93*, 269–310. [CrossRef]

11. Haida, M.; Banasiak, K.; Smolka, J.; Hafner, A.; Eikevik, T.M. Experimental analysis of the R744 vapour compression rack equipped with the multi-ejector expansion work recovery module. *Int. J. Refrig.* **2016**, *64*, 93–107. [CrossRef]
12. Purohit, N.; Gullo, P.; Dasgupta, M.S. Comparative assessment of low-GWP based refrigerating plants operating in hot climates. *Energy Procedia* **2017**, *109*, 138–145. [CrossRef]
13. Karampour, M.; Sawalha, S. State-of-the-art integrated CO_2 refrigeration system for supermarkets: A comparative analysis. *Int. J. Refrig.* **2018**, *86*, 239–257. [CrossRef]
14. Catalán-Gil, J.; Sánchez, D.; Llopis, R.; Nebot-Andrés, L.; Cabello, R. Energy Evaluation of Multiple Stage Commercial Refrigeration Architectures Adapted to F-Gas Regulation. *Energies* **2018**, *11*, 1915. [CrossRef]
15. Catalán-Gil, J.; Nebot-Andrés, L.; Sánchez, D.; Llopis, R.; Cabello, R.; Calleja-Anta, D. Improvements in CO_2 Booster Architectures with Different Economizer Arrangements. *Energies* **2020**, *13*, 1271. [CrossRef]
16. Mitsopoulos, G.; Syngounas, E.; Tsimpoukis, D.; Bellos, E.; Tzivanidis, C.; Anagnostatos, S. Annual performance of a supermarket refrigeration system using different configurations with CO_2 refrigerant. *Energy Convers. Manag. X* **2019**, *1*, 100006. [CrossRef]
17. Bellos, E.; Tzivanidis, C. A comparative study of CO_2 refrigeration systems. *Energy Convers. Manag. X* **2019**, *1*, 100002. [CrossRef]
18. Dai, B.; Qi, H.; Liu, S.; Zhong, Z.; Li, H.; Song, M.; Ma, M.; Sun, Z. Environmental and economical analyses of transcritical CO_2 heat pump combined with direct dedicated mechanical subcooling (DMS) for space heating in China. *Energy Convers. Manag.* **2019**, *198*, 111317. [CrossRef]
19. Bellos, E.; Tzivanidis, C. Enhancing the performance of a CO_2 refrigeration system with the use of an absorption chiller. *Int. J. Refrig.* **2019**, *108*, 37–52. [CrossRef]
20. Suamir, N. Integration of Trigeneration and CO_2 Based Refrigeration Systems for Energy Conservation. Ph.D. Thesis, Brunel University, London, UK, 2012. Available online: http://citeseerx.ist.psu.edu/viewdoc/download?doi=10.1.1.427.199&rep=rep1&type=pdf (accessed on 19 June 2020).
21. Aprea, C.; Greco, A.; Maiorino, A. The application of a desiccant wheel to increase the energetic performances of a transcritical cycle. *Energy Convers. Manag.* **2015**, *89*, 222–230. [CrossRef]
22. Mazzola, D.; Sheehan, J.; Bortoluzzi, D.; Smitt, G.; Orlandi, M. Supermarket application. Effects of sub-cooling on real R744 based trans-critical plants in warm and hot climate. Data analysis. In Proceedings of the 12th IIR Gustav Lorentzen Natural Working Fluids Conference, Edinburgh, UK, 21–24 August 2016; pp. 551–558.
23. Llopis, R.; Nebot-Andrés, L.; Sánchez, D.; Catalán-Gil, J.; Cabello, R. Subcooling methods for CO_2 refrigeration cycles: A review. *Int. J. Refrig.* **2018**, *93*, 85–107. [CrossRef]
24. Brown, T. Refrigeration System with Subcooler. U.S. Patent No. US3852974A, 13 August 1973.
25. Couvillion, R.J.; Larson, M.W.; Somerville, M.H. Analysis of a vapour-compression refrigeration system with mechanical subcooling. *ASHRAE Trans.* **1988**, *94*, 641–660.
26. Thornton, J.W.; Klein, S.A.; Mitchell, J.W. Dedicated mechanical subcooling design straregies for supermarket applications. *Int. J. Refrig.* **1997**, *17*, 508–515. [CrossRef]
27. Boiarski, M.; Podchernyaev, O.; Yudin, B.; Giguere, D. Enhancement of supermarket freezers to reduce energy consumption and increase refrigeration capacity. In Proceedings of the International Refrigeration and Air Conditioning Conference, Purdue, West Lafayette, IN, USA, 14–17 July 2000. Available online: http://docs.lib.purdue.edu/iracc/422 (accessed on 19 June 2020).
28. Benouali, J.; Chang, Y.S.; Clodic, D. Analysis of the sub-cooling on refrigerating systems using R410A or R404A. In Proceedings of the International Refrigeration and Air Conditioning Conference, Purdue, West Lafayette, IN, USA, 25–28 July 2000. Available online: http://docs.lib.purdue.edu/iracc/466 (accessed on 19 June 2020).
29. Khan, J.; Zubair, S.M. Design and rating of dedicated mechanical subcooling vapour compression refrigeration systems. *Proc. Inst. Mech. Eng. Part A* **2000**, *214*, 455–471. [CrossRef]
30. Qureshi, B.A.; Zubair, S.M. The effect of refrigerant combinations on performance of a vapor compression refrigeration system with dedicated mechanical sub-cooling. *Int. J. Refrig.* **2012**, *35*, 47–57. [CrossRef]
31. Qureshi, B.A.; Inam, M.; Antar, M.A.; Zubair, S.M. Experimental energetic analysis of a vapor compression refrigeration system with dedicated mechanical sub-cooling. *Appl. Energy* **2013**, *102*, 1035–1041. [CrossRef]

32. Brouwers, C.; Serwas, L. Market trends & developments for CO_2 in commercial refrigeration in Europe. In Proceedings of the EU Atmosphere Natural Refrigerants workshop, Brussels, Belgium, 5–7 November 2012. Available online: http://www.r744.com/knowledge/papersView/market_trends_amp_developments_for_co2_in_commercial_refrigeration_in_europe (accessed on 19 June 2020).
33. Frigo Consulting. Carrefour Alzira (ES). Most Southerly CO_2 Refrigeration System in Spain Now in Operation. 2013. Available online: http://www.r744.com/articles/5074/span_style_color_rgb_255_0_0_update_span_part_1_first_100_co_sub_2_sub_cooling_installation_in_southern_spain_carrefour_alzira_achieves_10_energy_savings (accessed on 19 June 2020).
34. She, X.; Yin, Y.; Zhang, X. A proposed subcooling method for vapour compression refrigeration cycle based on expansion power recovery. *Int. J. Refrig.* **2014**, *43*, 50–61. [CrossRef]
35. Hafner, A.; Hemmingsen, A.K. R744 refrigeration technologies for supermarkets in warm climates. In Proceedings of the 24th IIR International Congress of Refrigeration, Yokohama, Japan, 16–22 August 2015; pp. 125–133.
36. Llopis, R.; Cabello, R.; Sánchez, D.; Torrella, E. Energy improvements of CO_2 transcritical refrigeration cycles using dedicated mechanical subcooling. *Int. J. Refrig.* **2015**, *55*, 129–141. [CrossRef]
37. Sánchez, D.; Catalán-Gil, J.; Llopis, R.; Nebot-Andrés, L.; Cabello, R.; Torrella, E. Improvements in a CO_2 transcritical plant working with two different subcooling systems. *Refrig. Sci. Technol.* **2016**, 1014–1022. [CrossRef]
38. Nebot-Andrés, L.; Llopis, R.; Sánchez, D.; Cabello, R. Experimental evaluation of a dedicated mechanical subcooling system in a CO_2 transcritical refrigeration cycle. In Proceedings of the 12th Gustav Lorentzen Natural Working Fluids Conference, At Edinburgh, UK, 21–24 August 2016; pp. 965–972.
39. Cabello, R.; Sánchez, D.; Patiño, J.; Llopis, R.; Torrella, E. Experimental analysis of energy performance of modified single-stage CO_2 transcritical vapour compression cycles based on vapour injection in the suction line. *Appl. Therm. Eng.* **2012**, *47*, 86–94. [CrossRef]
40. Eikevik, T.M.; Bertelsen, S.; Haugsdal, S.; Tolstorebrov, I.; Jensen, S. CO_2 refrigeration system with integrated propan subcooler for supermarkets in warm climate. *Refrig. Sci. Technol.* **2016**, 211–218. [CrossRef]
41. Bush, J.; Beshr, M.; Aute, V.; Radermacher, R. Experimental evaluation of transcritical CO_2 refrigeration with mechanical subcooling. *Sci. Technol. Built Environ.* **2017**, *23*, 1013–1025. [CrossRef]
42. Dai, B.; Liu, S.; Ma, Y. Thermodynamic performance analysis of CO_2 transcritical refrigeration cycle assisted with mechanical subcooling. *Energy Procedia* **2017**, *105*, 2033–2038. [CrossRef]
43. Dai, B.; Liu, S.; Li, H.; Sun, Z.; Song, M.; Yang, Q.; Ma, Y. Energetic performance of transcritical CO_2 refrigeration cycles with mechanical subcooling using zeotropic mixtures as refrigerant. *Energy* **2018**, *150*, 205–221. [CrossRef]
44. Liu, S.; Lu, F.; Dai, B.; Nian, V.; Li, H.; Qi, H.; Li, J. Performance analysis of two-stage compression transcritical CO_2 refrigeration system with R290 mechanical subcooling unit. *Energy* **2019**, *189*, 116–143. [CrossRef]
45. Lemmon, E.W.; Huber, M.L.; McLinden, M.O. *Reference Fluid Thermodynamic and Transport Properties (REFPROP)*; NIST Standard Reference Database 23, v.9.1; National Institute of Standards: Gaithersburg, MD, USA, 2013.
46. ASHRAE Handbook—Fundamentals (SI Edition). *American Society of Heating, Refrigerating and Air Conditioning Engineers*, 2005 ed.; ASHRAE: Englewood, CO, USA, 2005.
47. Moffat, R.J. Describing the uncertainties in experimental results. *Exp. Therm. Fluids Sci.* **1988**, *1*, 3–17. [CrossRef]
48. Liao, S.M.; Zhao, T.S. Measurements of heat transfer coefficients from supercritical carbon dioxide flowing in horizontal min/micro channels. *J. Heat Transf.* **2002**, *124*, 413–420. [CrossRef]
49. Torrella, E.; Sánchez, D.; Llopis, R.; Cabello, R. Energetic evaluation of an internal heat exchanger in a CO_2 transcritical refrigeration plant using experimental data. *Int. J. Refrig.* **2011**, *34*, 40–49. [CrossRef]
50. Purohit, N.; Gupta, D.K.; Dasgupta, M.S. Experimental investigation of a CO_2 trans-critical cycle with IHX for chiller applications and its energetic and exergetic evaluation in warm climate. *Appl. Therm. Eng.* **2018**, *136*, 617–632. [CrossRef]
51. Sánchez, D.; Patiño, J.; Llopis, R.; Cabello, R.; Torrella, E.; Vicente Fuentes, F. New positions for an internal heat exchanger in a CO_2 supercritical refrigeration plant. Experimental analysis and energetic evaluation. *Appl. Therm. Eng.* **2014**, *63*, 129–139. [CrossRef]

52. Cabello, R.; Sánchez, D.; Llopis, R.; Torrella, E. Experimental evaluation of the energy efficiency of a CO_2 refrigerating plant working in transcritical conditions. *Appl. Therm. Eng.* **2008**, *28*, 1596–1604. [CrossRef]
53. Sánchez, D.; Cabello, R.; Llopis, R.; Torrella, E. Development and validation of a finite element model for water-CO_2 coaxial gas-coolers. *Appl. Energy* **2012**, *93*, 637–647. [CrossRef]
54. Sánchez, D.; Torrella, E.; Cabello, R.; Llopis, R. Influence of the superheat associated to a semihermetic compressor of a transcritical CO_2 refrigeration plant. *Appl. Therm. Eng.* **2010**, *30*, 302–309. [CrossRef]
55. ANSI/ASHRAE. *Designation and Safety Classification of Refrigerants*; Standard 34-2013; ANSI/ASHRAE: Georgia, GA, USA, 2013; ISSN 1041-2336.
56. IPCC. *Climate Change 2013: The Physical Science Basis. Contribution of Working Group I to the 5thAssessment Report of the Intergovernmental Panel on Climate Chang*, 1st ed.; Cambridge University Press: New York, NY, USA, 2013.
57. Sánchez, D.; Cabello, R.; Llopis, R.; Arauzo, I.; Catalán-Gil, J.; Torrella, E. Energy performance evaluation of R1234yf, R1234ze(E), R600a, R290 and R152a as low-GWP R134a alternatives. *Int. J. Refrig.* **2017**, *74*, 269–282. [CrossRef]
58. Boudreau, P.J. *The Compressor Operating Envelope*; Mechanical Business: Oakville, ON, Canada, 2013; pp. 80–81. Available online: http://www.r744.com/knowledge/papersView/the_compressor_operating_envelope (accessed on 19 June 2020).